FREE VIBRATION ANALYSIS OF FUNCTIONALLY GRADED PLATES USING HIGHER ORDER SHEAR DEFORMATION THEORY (HSDT)

A Thesis

Submitted by

Aritra Chanda

(Class roll: 002010402001)

(Exam Roll: M4CIV22001)

(Registration No: 153957 of 2020-2021)

Master of Engineering

IN

Civil Engineering

(Structural Engineering)

Under the guidance of

Dr Sreyashi Das

Department of Civil Engineering

Jadavpur University

Kolkata:- 700032

June 2022

Department of Civil Engineering

Faculty of Engineering and Technology

Jadavpur University

Kolkata- 700032

CERTIFICATE OF RECOMMENDATION

This is to certify that the thesis entitled, "**STATIC AND FREE VIBRATION ANALYSIS OF FUNCTIONALLY GRADED PLATE**" submitted by **Aritra Chanda**, Class Roll: 002010402001, Exam roll: M4CIV22001 and Registration number: 153957 of 2020-2021, in partial fulfilment of the requirements for the award of Master of Engineering degree in Civil Engineering with specialization in "Structural Engineering" at Jadavpur University, Kolkata is an authentic work carried out by him under my supervision and guidance.

I hereby recommend that the thesis is be accepted in partial fulfilment of the requirements for awarding the degree of **"Master of Engineering in Civil Engineering (Structural Engineering)"**.

_____

Dr.Sreyashi Das   Department of Civil Engineering
Associate Professor   Jadavpur University
Kolkata-700032

Countersigned by

_____

Dr Shibnath Chakraborty
Head of the Department
Department of Civil Engineering
Jadavpur University
Kolkata- 700032

Department of Civil Engineering

Faculty of Engineering and Technology

Jadavpur University

Kolkata- 700032

CERTIFICATE OF APPROVAL

This thesis paper is hereby approved as a credible study of an engineering subject carried out and presented in a manner satisfactorily to warrant its acceptance as a pre-requisite for the degree for which it has been submitted. It is understood that, by this approval the undersigned do not necessarily endorse or approve any statement made, opinion expressed or conclusion drawn therein but approved the thesis paper only for the purpose for which it is submitted.

Committee of Thesis Paper Examiners

_____
Signature of Examiner

_____
Signature of Examiner

DECLARATION

I, Aritra Chanda, Master of Engineering in Civil Engineering (Structural Engineering), Jadavpur University, Faculty of Engineering & Technology, hereby declare that the work being presented in the thesis work entitled, "**STATIC AND FREE VIBRATION ANALYSIS OF FUNCTIONALLY GRADED PLATE**" is an authentic record of the work that has been carried out at the Department of Civil Engineering, Jadavpur University, Kolkata under Dr Sreyashi Das, Associate professor, Department of Civil Engineering, Jadavpur University. The work contained in the thesis has not yet been submitted in part or full to any other university or institution or professional body for award of any degree or diploma or any fellowship.

_____

Place: Kolkata

Date:

Exam Roll: M4CIV22001

Regist.No.:153957 of 2020-2021

Aritra Chanda

Class Roll: 002010402001

ACKNOWLEDGEMENT

I am deeply indebted to **Dr. Sreyashi Das,** Associate Professor of Civil Engineering Department, my advisor and guide, for the motivation, guidance and patience throughout the thesis work. I appreciate her broad range of expertise and attention as well as the constant encouragement she has given me over the years. There is no need to mention that a big part of this thesis is the result of joint work with her, without which the completion of the work would have been impossible.

I am grateful to **Prof. Shibnath Chakraborty**, Head of the Department of Civil Engineering for his valuable suggestions and necessary help for the research work. I am grateful for friendly atmosphere of the Civil Engineering Division and all kind and helpful professors that I have met during my course. I would like to thank my parents; without their love, patience and support, I could not have completed this work.

Finally, I wish to thank many friends for the encouragement during these difficult years especially Kanchan Mandal, Akash Hossain, Arnab Samanta, Sukayan Sarkar, and Rehan Ahmed

_____

Place: Kolkata   Aritra Chanda

Date: Class Roll: 002010402001

ExamRoll: M4CIV22001

Regist. No.: 153957 of 2020-2021

ABSTRACT

A Functionally graded plate is made up of composite materials, microscopically inhomogeneous, in which the mechanical properties vary smoothly and continuously from one surface to another. It is a type of advanced materials in the field of composites, which can resist high temperatures and are proficient in reducing the thermal stresses. Functionally graded plates are becoming very popular in modern structural design as it allows excellent mechanical performance at minimal weight resulting higher payloads, increased range and decreased fuel consumption. FGMs are widely used to benefit a wide range of industries and have applications in industries like aerospace, transportation and nuclear industry.

In this paper the free vibration behaviour of FGM pates is being provided. A programme has been developed using MATLAB. The material properties at any particular depth have been modelled following the power law. Third order transverse shear deformation is accounted along with eight noded serendipity plate finite elements. To implement the theory a suitable C^0 continuous serendipity iso-parametric finite element with 7 degrees of freedom (DOFs) per node is proposed in order to reduce the computational efforts required in the formation of element matrices without affecting the solution accuracy. Numerical results have been presented for ceramic–metal graded plates with different boundary conditions. The convergence and validation studies manifest the accuracy and precision of the present proposed method. Parametric studies have been conducted by incorporating variation in support conditions, side to thickness ratio and different materials. Some results are presented in the form of tables and figures, which can suit as a benchmark for the future research.

TABLE OF CONTENTS

LIST OF FIGURES

LIST OF TABLES

Chapter 1

1.0 Introduction

Functionally graded materials (FGMs) are composite materials, microscopically inhomogeneous, in which the mechanical properties vary smoothly and continuously from one surface to another, and it finds application in various outlets of industry. It is the advanced materials in the field of composites, which can resist high temperatures and are proficient in reducing the thermal stresses. Functionally graded composite materials are of fascinating interest among design engineers since structural component properties can be designed and customized into finished parts through processing. The controlled variable is the concentration of reinforcing particles at various points within the component. While in locally isotropic materials , the volume fractions can be made to vary in a controlled manner from point to point the overall properties of FGM are unique and different from any of the individual material that forms it.
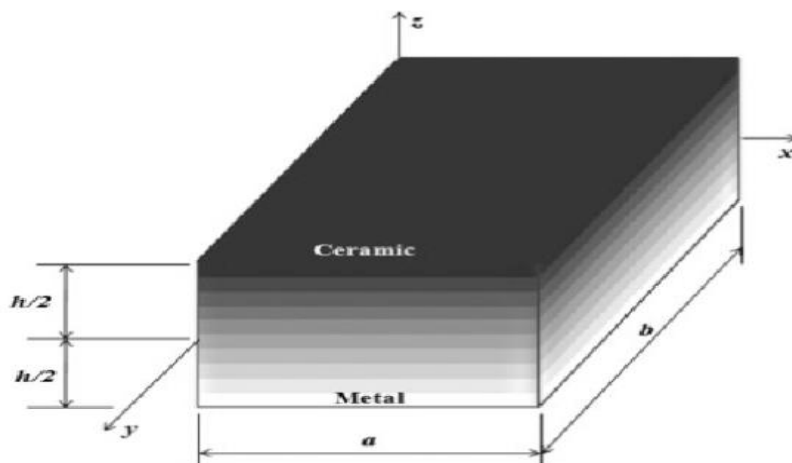
Fig 1: A typical FGM plate with ceramic on top and metal at bottom

1.1 History and first applications of functionally graded composites

Functionally graded materials (FGMs) are known for its tailor-made properties which are achieved through the continuous gradation of material phase from one surface to another. Due to FGMs being involved in the classification of composite materials, the material compositions of FGMs are assumed to vary smoothly and continuously throughout the gradient directions. The earliest FGMs were introduced by Japanese scientists in the mid-1980s as ultra-high temperature resistant materials for aerospace applications.

The concept of functionally graded materials (FGMs) was first enunciated in 1984 by a group of material scientists in Japan during a space plane project in the form of thermal barrier material which can withstand a huge temperature fluctuation across a very thin cross section(Koizumi,1993; Loy et al., 1999). Since then, FGMs have received major attention as heat-shielding advanced structural materials in various engineering applications and in

manufacturing industries, viz. aerospace, nuclear reactor, automobile, aircrafts, space vehicles, and biomedical and steel industries

1.2 Application of functionally graded (FG) composites

FGMs have received major attention as heat-shielding advanced structural materials in various engineering applications and in manufacturing industries, viz. aerospace, nuclear reactor, automobile, aircrafts, space vehicles, and biomedical and steel industries. FGMs were initially designed as thermal barrier materials for aerospace structures and fusion reactors (Hirai and Chen, 1999). The current focus of materials development activities for both composites and FGMs includes improvements in material performance, ability to support optimized structural designs, continued lowering of manufacturing costs, and ability to perform reliably in service. Two different possibilities of gradation behavior may be observed in the case of FG composites (i) continuous gradation of two different material phases from one interface to another and (ii) the change of material phases in a discontinuous (or stepwise) pattern is called segmented FGMs.

Due to gradation of material properties and thermal resistance behavior, there are a wide variety of applications of these materials in different sectors:

• **Automobiles:** Combustion chambers (SiC-SiC), engine cylinder liners (Al-SiC), CNG storage cylinders, diesel engine pistons (SiCw/Al- alloy), brake rotors, leaf springs (E-glass/epoxy), drive shafts (Al-C), motorcycle drive sprocket, pulleys, torque converter reactors, shock absorbers (SiCp/Al-alloy), radiator end caps.

• **Sub-marine:** Propulsion shaft (carbon and glass fibers), cylindrical pressure hull (graphite/epoxy), sonar domes (glass/epoxy), composite piping systems, scuba diving cylinders (Al-SiC), floats, boat hulls.

• **Commercial and industrial**: Pressure vessels, fuel tanks, cutting tool inserts, laptop cases, wind turbine blades, electric motors, fire fighting air bottles, artificial ligaments, MRI scanner cryogenic tubes, wheelchairs, hip joint implants, eyeglass frames, camera tripods, musical instruments, drilling motor shafts, drill casings, crane components, high-pressure hydraulic pipes, X-ray tables, heart valves, helmets, crucibles, beams.

• **Aerospace equipment and structures**: Rocket nozzles (TiAl-SiC fibers), heat exchanger panels, engine parts (Be-Al), wind tunnel blades, space- craft truss structures, reflectors, solar panels, camera housings, hubble space telescope metering truss assembly, turbine wheels (operating above 40,000 rpm), nose caps, and leading edge of missiles and space shuttle.

• **Aerospace:** Wings, rotary launchers, engine casings, rings (Al2O3/Al- alloy), drive shafts, propeller blades, landing gear doors, thrust reversers (carbon/bismaleimide), helicopter components, viz. rotor drive shafts, mast mounts, main rotor blades (carbon/epoxy).

• **Sports:** Racing bicycle frames (SiCw/6061), racing vehicle frames.

1.3 Benefits of FGM

1. FGM as an interface layer to connect two incompatible materials can greatly enhance the bond strength.

2. FGM coating and interface can be used to reduce the residual stress and thermal stress.

3. FGM coating can be used to connect the materials to eliminate the stress at the interface and end point stress singularity.

4. FGM coating not only enhances the strength of the connections but can also reduce the crack driving force.

5. FGM has the ability to control deformation, dynamic response, wear, corrosion etc.

6. FGM also provides the opportunities to take the benefits of different material systems e.g., ceramics and metals.

7. Ceramic part has good thermal resistance, wear and oxidation (rust) resistance whereas metallic part has superior fracture toughness, high strength and bonding capability.

8. FGM has wide range of applications in dental and orthopaedic applications for teeth and bone replacement.

9. FGM are used in energy conversion devices. They also provide thermal barrier and used as protective coating on turbine blades in gas turbine engine.

1.4 Demerits of FGM

1. A proper database of graded material (including material system, parameters, material preparation and performance evaluation) is to be developed.

2. Still need further research and examination on the physical properties of the material model. Microscopic structure and the quantitative relationship between preparation conditions to be established in order to accurately and reliably predict the physical properties of graded materials.

3. Research should focus on variation of gradient material with respect to thermal stress relaxation of the material as well as keep the road open to variety of engineering applications.

4. Still need to improve the continuum theory, quantum (discrete) theory, percolation theory and micro-structure model, and rely on computer simulation of the material properties for theoretical prediction particular.

5. Functionally graded materials prepared are samples of small size, simple structure. More practical valued materials still need to be developed.

6. The total preparation costs are high.

Chapter 2

2.0 Literature review

Many literatures are available in this topic of functionally graded materials. Besides a lot of research needs to be done on this topic.

We have discussed a few literature given below

1. **Author- M.N.A. Gulshan Taj, Anupam Chakrabarti , Abdul Hamid Sheikh**

   Applied Mathematical Modelling (Volume 37, Issues 18–19, 1 October 2013, Pages 8484-8494)

Topic- **Analysis of functionally graded plates using higher order shear deformation theory**

About topic - This work addresses a static analysis of functionally graded material (FGM) plates using higher order shear deformation theory. In the theory the transverse shear stresses are represented as quadratic through the thickness and hence it requires no shear correction factor. The material property gradient is assumed to vary in the thickness direction. Mori and Tanaka theory (1973) [1] is used to represent the material property of FGM plate at any point. The thermal gradient across the plate thickness is represented accurately by utilizing the thermal properties of the constituent materials. Results have been obtained by employing a C^0 continuous iso parametric Lagrangian finite element with seven degrees of freedom for each node. The convergence and comparison studies are presented and effects of the different material composition and the plate geometry (side-thickness, side–side) on deflection and temperature are investigated. Effect of skew angle on deflection and axial stress of the plate is also studied. Effects of material constant n on deflection and the temperature distribution are also discussed in detail.

2. **Author - Ashraf M. Zenkour(Applied Mathematical Modelling)**

   Volume 37, Issues 20–21, 1 November 2013, Pages 9041-9051

Topic - **A simple four-unknown refined theory for bending analysis of functionally graded plates**

About topic - In the present paper, a refined trigonometric higher-order plate theory is simply derived which satisfies the free surface conditions. Moreover, the number of unknowns of this theory is the least one comparing with other shear theories. The effects of transverse shear strains as well as the transverse normal strain are taken into account. The number of unknown functions involved in the present theory is only four as against six or more in case of other shear and normal deformation theories. The bending response of FG rectangular plates is presented. A comparison with the corresponding results is made to check the accuracy and efficiency of the present theory. Additional results for all displacements and stresses are investigated through-the-thickness of the FG rectangular plate

3. **Authors – Andrea Apuzzo, Raffaele Barreta and Raimondo Luciano(Composites Part B: Engineering,Volume 68, January 2015, Pages 266-269)**

Topic - Some analytical solutions of functionally graded Kirchhoff plates

About topic - The elastostatic problem of a functionally graded Kirchhoff plate, with no kinematic constraints on the boundary, under constant distributions of transverse loads per unit area and of boundary bending couples is investigated. Closed-form expressions are provided for displacements, bending–twisting curvatures and moments of an isotropic plate with elastic stiffness and boundary distributed shear forces, assigned respectively in terms of the stress function and of its normal derivative of a corresponding Saint-Venant beam under torsion. The methodology is adopted to solve circular plates with local and Eringen-type elastic constitutive behaviors, providing thus new benchmarks for computational mechanics. The proposed approach can be used to obtain other exact solutions for plates whose planform coincides with the cross-section of beams for which the Prandtl stress function is known in an analytical form.

4. **Authors – Thuc P.Vo , Hu Tai-Thai , Trung Kien Nangyuen , Fawad Inam(Composites Part B: Engineering) Volume 68, January 2015, Pages 59-74**

Topic - Static behaviour of functionally graded sandwich beams using a quasi-3D theory

About topic - This paper presents static behaviour of functionally graded (FG) sandwich beams by using a quasi-3D theory, which includes both shear deformation and thickness stretching effects. Various symmetric and non-symmetric sandwich beams with FG material in the core or skins under the uniformly distributed load are considered. Finite element model (FEM) and Navier solutions are developed to determine the displacement and stresses of FG sandwich beams for various power-law index, skin-core-skin thickness ratios and boundary conditions. Numerical results are compared with those predicted by other theories to show the effects of shear deformation and thickness stretching on displacement and stresses.

5. **Authors – Amale Mahi , El Abbas Adda Bedia , Abdelouahed Tounsi(Applied Mathematical Modelling) Volume 39, Issue 9, 1 May 2015, Pages 2489-2508**

Topic - A new hyperbolic shear deformation theory for bending and free vibration analysis of isotropic, functionally graded, sandwich and laminated composite plates

About Topic - A new hyperbolic shear deformation theory applicable to bending and free vibration analysis of isotropic, functionally graded, sandwich and laminated composite plates is presented. This new theory has five degrees of freedom, provides parabolic transverse shear strains across the thickness direction and hence, it does not need shear correction factor. Moreover, zero-traction boundary conditions on the top and bottom surfaces of the plate are satisfied rigorously. The energy functional of the system is obtained using Hamilton's principle. Analytical solutions of deflection and stresses are obtained using Navier-type procedure. Free vibration frequencies are then accurately calculated using a set of boundary characteristic orthogonal polynomials associated with Ritz method. Numerical comparisons are conducted to verify and to demonstrate the accuracy and efficiency of the present theory. Excellent agreement with the known results in the literature has been obtained.

6. **Authors - Alibeigloo(European Journal of Mechanics - A/Solids) Volume 44, March–April 2014, Pages 104-115**

Topic - Free vibration analysis of functionally graded carbon nanotube-reinforced composite cylindrical panel embedded in piezoelectric layers by using theory of elasticity

About topic - In this paper free vibration behavior of functionally graded carbon nanotube-reinforced composite (FG-CNTRC) cylindrical panel embedded in piezoelectric layers with simply supported boundary conditions is investigated by using three-dimensional theory of elasticity. By using Fourier series expansion along the longitudinal and latitudinal directions and state space technique across the thickness direction, state space differential equations are solved analytically. The traction-free surface conditions then give rise to the characteristic equation for natural frequencies. Accuracy and convergence of the present approach are validated by comparing the numerical results with those found in literature. In addition, the effects of volume fraction of CNT, four cases of FG-CNTRC, piezoelectric layer thickness, mid radius to thickness ration and modes number on the vibration behavior of the hybrid cylindrical panel are also examined.

7. **Authors – PingZhu , Z.X.Lei , K.M.Liew(Composite Structures,Volume 94, Issue 4, March 2012, Pages 1450-1460)**

Topic - Static and free vibration analyses of carbon nanotube-reinforced composite plates using finite element method with first order shear deformation plate theory

About topic - This paper mainly presents bending and free vibration analyses of thin-to-moderately thick composite plates reinforced by single-walled carbon nanotubes using the finite element method based on the first order shear deformation plate theory. Four types of distributions of the uniaxially aligned reinforcement material are considered, that is, uniform and three kinds of functionally graded distributions of carbon nanotubes along the thickness direction of plates. The effective material properties of the nanocomposite plates are estimated according to the rule of mixture. Detailed parametric studies have been carried out to reveal the influences of the volume fractions of carbon nanotubes and the edge-to-thickness ratios on the bending responses, natural frequencies and mode shapes of the plates. In addition, the effects of different boundary conditions are also examined. Numerical examples are computed by an in-house finite element code and the results show good agreement with the solutions obtained by the FE commercial package ANSYS.

8. **Authors – Mohammad Talha, B.N. Singh (Applied Mathematical Modelling 34 (2010) 3991–4011)**

Topic - Static response and free vibration analysis of FGM plates using higher order shear deformation theory

About topic - Free vibration and static analysis of functionally graded material (FGM) plates are studied using higher order shear deformation theory with a special modification in the transverse displacement in conjunction with finite element models. The mechanical properties of the plate are assumed to vary continuously in the thickness direction by a simple power-law

distribution in terms of the volume fractions of the constituents. The fundamental equations for FGM plates are derived using variational approach by considering traction free boundary conditions on the top and bottom faces of the plate. Results have been obtained by employing a continuous isoparametric Lagrangian finite element with 13 degrees of freedom per node. Convergence tests and comparison studies have been carried out to demonstrate the efficiency of the present model. Numerical results for different thickness ratios, aspect ratios and volume fraction index with different boundary conditions have been presented. It is observed that the natural frequency parameter increases for plate aspect ratio, lower volume fraction index n and smaller thickness ratios. It is also observed that the effect of thickness ratio on the frequency of a plate is independent of the volume fraction index. For a given thickness ratio non-dimensional deflection increases as the volume fraction index increases. It is concluded that the gradient in the material properties plays a vital role in determining the response of the FGM plates.

9. **Authors – J.N Reddy, INTERNATIONAL JOURNAL FOR NUMERICAL METHODS IN ENGINEERING Int. J. Numer. Meth. Engng. 47, 663-684(2000)**

Topic - Analysis of functionally graded plates

About topic - Theoretical formulation, Navier's solutions of rectangular plates, and finite element models based on the third-order shear deformation plate theory are presented for the analysis of through-thickness functionally graded plates. The plates are assumed to have isotropic, two-constituent material distribution through the thickness and the modulus of elasticity of the plate is assumed to vary according to a power-law distribution in terms of the volume fractions of the constituents. The formulation accounts for the thermomechanical coupling, time dependency, and the Von Karman-type geometric non-linearity. Numerical results of the linear third-order theory and non-linear first-order theory are presented to show the effect of the material distribution on the deflections and stresses.

2.1 Objective

In our thesis, we have used third-order shear deformation theory and have solved the problem using the finite element method with the aid of MATLAB. Eight noded isoparametric serendipity plate bending elements have been used. Young's modulus and density per unit volume are assumed to vary continuously and smoothly through the plate thickness according to a power-law distribution. Parametric studies have been done for different materials, thickness to length ratios, support conditions and power-law indices.

Chapter 3

3.0 Theoretical Background

3.1 Dynamic equation

In the case of a rigid body, only Newton's second law of motion is adequate to derive the laws of motion but in the case of a deformable continuum, the governing dynamic equation of the elastic body is derived from D'Alembert's principle. D'Alembert's principle gives an alternative way to describe the second law of motion:

$$\vec{F} - m\vec{a} = 0 \quad\quad\quad (3.1.1)$$

Where $\vec{F}$ and $\vec{a}$ are the force and acceleration acting on mass m respectively. And $m\vec{a}$ is the inertial pseudo force acting on the mass.

From the principle of virtual displacement, the following relation (3.1.2) arises and it is valid for static equilibrium.

$$\iiint_v B_i \delta u_i dV + \oiint_s T_i^n \delta u_i dS - \iiint_v \sigma_{ij} \delta\varepsilon_{ij} dV = 0 \quad\quad\quad (3.1.2)$$

Equation (3.1.2) can be generalized by adding term $(-\iiint_v \frac{\partial^2 u_i}{\partial t^2} \delta u_i dV)$ to the left-hand side for the dynamic condition. Body force and Traction force on the body volume V and surface S in this equation is mentioned by B and T in eq. 3.1.2. Now for virtual displacement δu_i at time t eq. 3.1.2 can be extended as:

$$-\iiint_v \frac{\partial^2 u_i}{\partial t^2} \delta u_i dV + \iiint_v B_i \delta u_i\, dV + \oiint_s T_i^n \delta u_i dS - \iiint_v \sigma_{ij} \delta\varepsilon_{ij}\, dV = 0 \quad\quad\quad (3.1.3)$$

With Inertia considered as a distributed body force, eq. 3.1.3 is the statement of the principle of virtual work. At a point or node, the displacement vector u_i generally consist of six number of displacement degree of freedom. The displacement D.O.F. in vector form can be present as

$$\{u\} = \left\{ u \;\; v \;\; w \;\; \theta_x \theta_y \; \theta_z \right\}^T \qu\quad\quad (3.1.4)$$

Now the eq. 3.1.3 in matrix form is as follows:

$$-\iiint_v \{\delta u\}^T [\rho] \{\ddot{u}\}\, dV + \iiint_v \{\delta u\}^T \{B\}\, dV + \oiint_s \{\delta u\}^T \{T\}\, dS - \iiint_v \{\delta\varepsilon\}^T \{\sigma\}\, dV = 0 \quad (3.1.5)$$

To accommodate the energy dissipation due to friction, δW_{diss} , eq. 3.1.5 can be further extended, where,

$$\delta W_{diss} = \delta \left(\iiint \{u\}^T \{f\} dV \right) \quad\quad\quad (3.1.6)$$

Here, $\{f\}$ is the dissipative force vector per unit volume. For the case of viscous damping, $\{f\}$ is proportional to the structural velocity, so that

$$\{f\} = C \{\dot{u}\} \quad\quad\quad (3.1.7)$$

Where C is a constant of proportionality.

Now the displacement $\{u\}$, at any point on the domain, approximated as

$$\{u\} = [N] \{d\} \quad\quad\quad (3.1.8)$$

Where $\{u\}$, is the array of required displacements anywhere on the structural domain, is interpolated from the nodal displacements. [N] is shape function and $\{d\}$ contains displacements at some predefined points on the structure. The interpolation function [N] and nodal displacement $\{d\}$ are assumed to be spatial and temporal functions respectively. Eq. 3.1.8 can be spatially differentiated, so that strain with nodal displacement relation can arise as

$\{\varepsilon\} = [B] \{d\}$ _____(3.1.9)

And the constitutive relation between strain and stress is written as

$\{\sigma\} = [D] \{\varepsilon\}$ _____(3.1.10)

Thus including damping eq. 3.1.5 can be expressed as-

$-\iiint \{\delta d\} [N]^T[\rho][N]\{\ddot{d}\}dV + \iiint \{\delta d\}^T [N]^T\{B\}dV + \oiint \{\delta d\}^T [N]^T\{T\}dS -$

$\iiint \{\delta d\}^T [N]^T C [N]\{\dot{d}\}dV - \iiint \{\delta d\}^T [B]^T[D][B]\{d\}dV = 0$ _____(3.1.11)

Since the virtual displacement $\{\delta d\}$ is arbitrary, eq. 3.1.11 can be modified and the final out coming is known as governing dynamic equation of the system,

$[M]\{\ddot{d}\} + [C]\{\dot{d}\} + [K]\{d\} = 0$ _____(3.1.12)

Where,

$[M] = \iiint [N]^T[\rho][N]\, dV = $ Mass Matrix _____(3.1.13)

$[K] = \iiint [B]^T[D][B]\, dV = $ Stiffness Matrix _____(3.1.14)

$[C] = \iiint [N]^T[C][N]\, dV = $ Damping Matrix _____(3.1.15)

$\{F\} = \iiint [N]^T\{B\}\, dV + \oiint [N]^T\{T\}\, dS = $ Force vector _____(3.1.16)

For the case of static equilibrium, the governing equation excludes the inertia and damping terms and the load becomes independent of time. For an un-damped free vibration problem, the damping and forcing terms are identically set to zero. Whereas, for an un-damped forced vibration the damping term is omitted from the Eq. (3.1.12). Thus, to summarize, the governing equations for various conditions are furnished as,

Bending problem:$[K]\{d\} = \{F\}$ _____(3.1.17)

Free vibration :$[M]\{\ddot{d}\} + [K]\{d\} = 0$ _____(3.1.18)

Undamped force vibration :$[M]\{\ddot{d}\} + [K]\{d\} = \{F\}$ _____(3.1.19)

Damped force vibration :$[M]\{\ddot{d}\} + [C]\{\dot{d}\} + [K]\{d\} = \{F\}$ _____(3.1.20)

We will use the eq. (3.1.18) for present analysis purpose.

3.2 Basic Elastic equation

The state of stress at a point in a continuous medium is represented by nine stress components σ_{ij} (where i,j = 1,2,3) at the sides of an elemental cube where 1-,2-,3- are axes of a reference coordinate system. Similarly, the state of deformation at a point is represented by ε_{ij}. For general case, the stress and strain components are related by generalised Hook's law.

$\sigma_{ij} = C_{ijkl}\varepsilon_{kl}$; (i,j,k,l=1,2,3) _____(3.2.1)

Where C_{ijkl} = Stiffness components

Hence a total of 81 elastic constants are required to characterize an anisotropic material fully. Now, from the law of conservation of linear momentum, we can find the equation of motion, which can be expressed as-

$\sigma_{ji,j} + B_i = \rho \ddot{u}_i$ _____(3.2.2)

Combining the eq.(3.2.1) and (3.2.2) and neglecting the body force term the equation of dynamic equilibrium can be represented as

$\rho \ddot{u}_i - (C_{ijkl}\varepsilon_{kl})_{,j} = 0$; (i,j,k,l=1,2,3) _____(3.2.3)

However, the number of independent elastic constants have been reduced to 36 due to symmetry of the stress and strain tensors, i.e., $\sigma_{ij}=\sigma_{ji}$ and $\varepsilon_{ij}=\varepsilon_{ji}$. The stress-strain relations for an anisotropic material can be written as

$$
\begin{bmatrix} \sigma_{xx} \text{ or } \sigma_1 \\ \sigma_{yy} \text{ or } \sigma_2 \\ \sigma_{zz} \text{ or } \sigma_3 \\ T_{yz} \text{ or } \sigma_4 \\ T_{zx} \text{ or } \sigma_5 \\ T_{xy} \text{ or } \sigma_6 \end{bmatrix} = \begin{bmatrix} C_{11} & C_{12} & C_{13} & C_{14} & C_{15} & C_{16} \\ C_{21} & C_{22} & C_{23} & C_{24} & C_{25} & C_{26} \\ C_{31} & C_{32} & C_{33} & C_{34} & C_{35} & C_{36} \\ C_{41} & C_{42} & C_{43} & C_{44} & C_{45} & C_{46} \\ C_{51} & C_{52} & C_{53} & C_{54} & C_{55} & C_{56} \\ C_{61} & C_{62} & C_{63} & C_{64} & C_{65} & C_{66} \end{bmatrix} \begin{bmatrix} \varepsilon_{xx} \\ \varepsilon_{yy} \\ \varepsilon_{zz} \\ \varepsilon_{yz} \\ \varepsilon_{zx} \\ \varepsilon_{xy} \end{bmatrix}
\tag{3.2.4}
$$

Or in indicial notation, $\sigma_i = C_{ij}\varepsilon_j$;(i,j,=1,2,...,6)

The work per unit volume is expressed as

$$
W = \frac{1}{2}C_{ij}\varepsilon_i\varepsilon_j
\tag{3.2.5}
$$

Where W is strain energy density function defined as the strain energy contained in a unit volume of the structure undergoing deformation from an arbitrary datum. The stress-strain relation can be obtained by differentiating eq.(3.2.5)

$$
\sigma_i = \frac{\partial W}{\partial \varepsilon_i} = C_{ij}\varepsilon_j
\tag{3.2.6}
$$

By differentiating again we obtain

$$
C_{ij} = \frac{\partial^2 W}{\partial \varepsilon_i \varepsilon_j}
\tag{3.2.7}
$$

Similarly, by reversing the order of differentiation, we can obtain

$$
C_{ji} = \frac{\partial^2 W}{\partial \varepsilon_j \varepsilon_i}
\tag{3.2.8}
$$

Eq. 3.2.7 and eq. 3.2.8 yields

$$
C_{ij} = C_{ji}
\tag{3.2.9}
$$

That is the stiffness matrix is symmetric. Thus the state of stress at a point can be written in terms of 21 independent elastic constants as shown in Eq. 3.2.10.

$$
\begin{bmatrix} \sigma_{xx} \text{ or } \sigma_1 \\ \sigma_{yy} \text{ or } \sigma_2 \\ \sigma_{zz} \text{ or } \sigma_3 \\ T_{yz} \text{ or } \sigma_4 \\ T_{zx} \text{ or } \sigma_5 \\ T_{xy} \text{ or } \sigma_6 \end{bmatrix} = \begin{bmatrix} C_{11} & C_{12} & C_{13} & C_{14} & C_{15} & C_{16} \\ C_{21} & C_{22} & C_{23} & C_{24} & C_{25} & C_{26} \\ C_{13} & C_{23} & C_{33} & C_{34} & C_{35} & C_{36} \\ C_{14} & C_{24} & C_{34} & C_{44} & C_{45} & C_{46} \\ C_{15} & C_{25} & C_{35} & C_{45} & C_{55} & C_{56} \\ C_{16} & C_{26} & C_{36} & C_{46} & C_{56} & C_{66} \end{bmatrix} \begin{bmatrix} \varepsilon_{xx} \\ \varepsilon_{yy} \\ \varepsilon_{zz} \\ \varepsilon_{yz} \\ \varepsilon_{zx} \\ \varepsilon_{xy} \end{bmatrix}
\tag{3.2.10}
$$

3.3 The rule of mixtures

A functionally graded material is composed by mixing two materials like metal and ceramic. Several macro mechanics models have been developed in the past to determine the variation in properties. The common model among all is the rule of mixtures. According to this model, an arbitrary material property P of the FGM is supposed to vary smoothly along a direction, as a function of the volume fractions and properties of the constituent materials. The varying direction is the thickness direction as here FG plates have been considered. P can represent, for example, the modulus of elasticity, the mass density, and/or Poisson's ratio. This property can be expressed as a linear combination

$P(z) = P_1V_1 + P_2V_2$ _____(3.3.1)

where z is the varying direction P_1, V_1 and P_2, V_2 are the material properties and volume fractions of the constituent materials 1 and 2, respectively. The volume fractions of all the constituent materials should add up to unity.

$V_1 + V_2 = 1$ _____(3.3.2)

The volume fraction V_1 is assumed to have the following power-law distribution,

$V_1 = [z/h + 1/2]^N$ _____(3.3.3)

where h = thickness of the plate; N = volume fraction exponent (positive real values which dictates the material variation profile through the thickness)

The constituent materials are normally taken as ceramic (material 1) and metal (material 2), respectively. The bottom surface, z = −h/2, of the functionally graded plate is pure metal and the top surface, z = +h/2, is pure ceramic. The material 2 content in the plate increases as the value of N increases. N = 0 and N = ∞ indicate a homogeneous plate of material 1 and material 2 respectively.
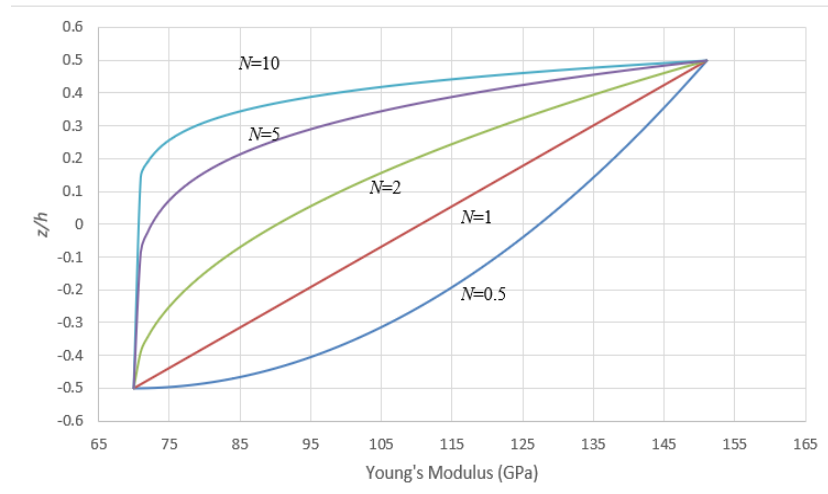
Figure 3.3.1 Power-law variation of Young's modulus of the FG plate

3.4 Free vibration analysis of (FG) plates using HSDT

3.4.1 Theoretical background

The determination of accurate behaviour of the FGMs largely depends on the theory used to model the structure because in the FGMs, material properties vary continuously as a function of position in the preferred direction. Various concepts have been developed to inculcate the appropriate analysis of the FGM plates. The classical Kirchhoff plate theory neglects transverse shear deformation and gives acceptable results for relatively thin plates. In order to circumvent this problem, earlier attempts were made by Reissner and Mindlin by using first order shear deformation theory. However, a shear-correction factor must be incorporated to overcome the

problem of a constant transverse shear stress distribution and its value depends on various parameters, such as applied loads, boundary conditions and geometric parameters, etc. The inaccuracy occurs due to neglecting the effects of transverse shear and normal strains in the plate. The first-order shear deformation theory proposed by Mindlin does not satisfy the parabolic variation of transverse shear strain in the thickness direction. Subsequently, many higher order theories were proposed.

The higher order theories assume the in-plane displacements as a cubic expression of the thickness coordinate and the out-of-plane displacement to be constant. Thus, the development of higher order shear deformation theory to assimilate the behaviour of FGM structures has been of high importance to the researchers.

3.4.2 Third Order Assumptions
The third order shear deformation theory is based on following assumptions

1. The material behaviour is linear and elastic.
2. The thickness, *t*, of the laminate is small compared to the other two dimensions.
3. Displacements *u*, *v*, and *w* are small compared to the laminate thickness, *h*.
4. Normal to the mid-plane before deformation does not remain straight and normal to the mid-plane after deformation. Hence this theory is termed as third order shear deformation theory.
5. Stresses normal to the mid-plane are neglected.
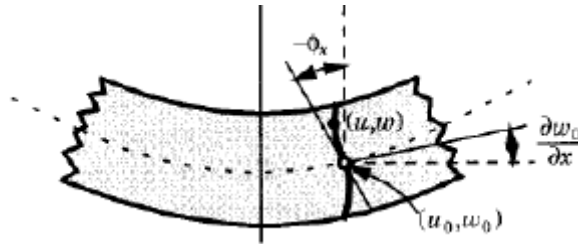
Fig 3.4.2a: Deformed shape of FGM plate under HSDT

3.4.3 Displacement Model
The in-plane displacements *u* and *v* of any point at any distance *z* from the mid-plane are given by:

$$u(x, y, z, t) = u_0(x, y, t) + z\Phi_x(x, y, t) + c_1 z^3(\Phi_x + w_{0,x}) \underline{\quad\quad}(i)$$

$$v(x, y, z, t) = v_0(x, y, t) + z\phi_y(x, y, t) + c_1 z^3(\Phi_y + w_{0,y}) \underline{\quad\quad}(ii)$$

The out plane displacement is given by w, which is a function of space coordinates and time

$$w(x, y, z, t) = w_0(x, y, t) \underline{\quad\quad\quad\quad\quad\quad}(iii)$$

Here Φ_x and Φ_y are the shear rotation angles of the transverse normal at mid plane (z=0) where as $w_{0,x}$ and $w_{0,y}$ are the transverse bending rotations. u_0, v_0 and w_0 are the mid plane displacements along x, y and z axis respectively. For Reddy's third order shear deformation theory $c_1 = {}^4\!/_{(3h^2)}$

3.4.4 Strain Displacement Relation

Since the assumptions made above restrict the model to small deflection and small strain regime the strains considered are of first order.

With the displacements, defined in Eq.(i)&(ii) the linear in-plane normal strains of FGM plate at a distance z from the mid-surface can be found out as,

$$\begin{Bmatrix} \varepsilon_{xx} \\ \varepsilon_{yy} \\ \gamma_{xy} \end{Bmatrix} = \begin{Bmatrix} \varepsilon_{xx}^0 \\ \varepsilon_{yy}^0 \\ \gamma_{xy}^0 \end{Bmatrix} + z \begin{Bmatrix} \varepsilon_{xx}^1 \\ \varepsilon_{yy}^1 \\ \gamma_{xy}^1 \end{Bmatrix} + z^3 \begin{Bmatrix} \varepsilon_{xx}^3 \\ \varepsilon_{yy}^3 \\ \gamma_{xy}^3 \end{Bmatrix}$$

Where $\begin{Bmatrix} \varepsilon_{xx}^0 \\ \varepsilon_{yy}^0 \\ \gamma_{xy}^0 \end{Bmatrix} = \begin{Bmatrix} u_{0,x} \\ v_{0,y} \\ u_{0,y} + v_{0,x} \end{Bmatrix}$; $\begin{Bmatrix} \varepsilon_{xx}^1 \\ \varepsilon_{yy}^1 \\ \gamma_{xy}^1 \end{Bmatrix} = \begin{Bmatrix} \Phi_{x,x} \\ \Phi_{y,y} \\ \Phi_{x,y} + \Phi_{y,x} \end{Bmatrix}$;

$$\begin{Bmatrix} \varepsilon_{xx}^3 \\ \varepsilon_{yy}^3 \\ \gamma_{xy}^3 \end{Bmatrix} = -c_1 \begin{Bmatrix} \Phi_{x,x} + w_{0,xx} \\ \Phi_{y,y} + w_{0,yy} \\ \Phi_{x,y} + \Phi_{y,x} + 2w_{0,xy} \end{Bmatrix}$$

Transverse shear strains are:

$$\begin{Bmatrix} \gamma_{yz} \\ \gamma_{xz} \end{Bmatrix} = \begin{Bmatrix} \gamma_{yz}^0 \\ \gamma_{xz}^0 \end{Bmatrix} + z^2 \begin{Bmatrix} \gamma_{yz}^2 \\ \gamma_{xz}^2 \end{Bmatrix}$$

Where $\begin{Bmatrix} \gamma_{yz}^0 \\ \gamma_{xz}^0 \end{Bmatrix} = \begin{Bmatrix} \Phi_y \\ \Phi_x \end{Bmatrix} + \begin{Bmatrix} w_{0,y} \\ w_{0,x} \end{Bmatrix}$; $\begin{Bmatrix} \gamma_{yz}^2 \\ \gamma_{xz}^2 \end{Bmatrix} = -\frac{4}{h^2} \begin{Bmatrix} \Phi_y + w_{0,y} \\ \Phi_x + w_{0,x} \end{Bmatrix}$

3.4.5 Stress Resultants and Constitutive Relations

Inserting the above relationship in constitutive relation form the following relation is obtained.

$$\begin{Bmatrix} \sigma_x \\ \sigma_y \\ \tau_{xy} \end{Bmatrix} = [c_{ij}] \begin{Bmatrix} \varepsilon_{xx} \\ \varepsilon_{yy} \\ \gamma_{xy} \end{Bmatrix} \qquad (i, j = 1,2,3)$$

$$= [c_{ij}] \left[\begin{Bmatrix} \varepsilon_{xx}^{(0)} \\ \varepsilon_{yy}^{(0)} \\ \gamma_{xy}^{(0)} \end{Bmatrix} + z \begin{Bmatrix} \varepsilon_{xx}^{(1)} \\ \varepsilon_{yy}^{(1)} \\ \gamma_{xy}^{(1)} \end{Bmatrix} + z^3 \begin{Bmatrix} \varepsilon_{xx}^{(3)} \\ \varepsilon_{yy}^{(3)} \\ \gamma_{xy}^{(3)} \end{Bmatrix} \right]$$

Transverse shear stresses:

$$\begin{Bmatrix} \tau_{xz} \\ \tau_{yz} \end{Bmatrix} = [c_{ij}] \begin{Bmatrix} \gamma_{xz} \\ \gamma_{yz} \end{Bmatrix} (i, j = 4, 5)$$

$$= [c_{ij}] \left[\begin{Bmatrix} \gamma_{yz}^{(0)} \\ \gamma_{xz}^{(0)} \end{Bmatrix} + z^2 \begin{Bmatrix} \gamma_{yz}^{(2)} \\ \gamma_{xz}^{(2)} \end{Bmatrix} \right]$$

Here constitutive coefficient c_{ij} varies along plate thickness 'h' so it's a function of 'z'

Therefore, $c_{11} = \frac{E(Z)}{1-v_1 v_2}$; $c_{22} = \frac{E(Z)}{1-v_1 v_2}$; $c_{12} = \frac{v_1 E(Z)}{1-v_1 v_2}$; $c_{66} = \frac{E(Z)}{2(1+v_1)}$; $c_{44} = \frac{E(Z)}{2(1+v_1)}$

$c_{55} = \frac{E(Z)}{2(1+v_1)}$ and E(z) is the Young's modulus which varies with thickness according to the

power law. $P(z) = (P_c - P_m)\left(\frac{z}{h} + \frac{1}{2}\right)^k + P_m$ where P(z) is any property of the FGM plate

Here shear correction factor α is not taken into account because the transverse shear distribution is not taken uniform throughout the cross section of the FGM plate. These expressions have to be integrated over the entire plate thickness to account for the FGM property. As a result the stress terms are replaced by the stress-resultant terms, while the conventional strain terms are replaced by the mid-plane strain terms.

Hence, the in-plane forces,

$$\begin{bmatrix} N_x \\ N_y \\ N_{xy} \end{bmatrix} = \int_{-h/2}^{h/2} \begin{bmatrix} \sigma_x \\ \sigma_y \\ \sigma_{xy} \end{bmatrix} dz$$

$$= \int_{-h/2}^{h/2} [c_{ij}] \begin{Bmatrix} \varepsilon_{xx} \\ \varepsilon_{yy} \\ \gamma_{xy} \end{Bmatrix} dz \quad for\ i,j = 1,2,3$$

$$= \int_{-h/2}^{h/2} [c_{ij}] \left[\begin{Bmatrix} \varepsilon_{xx}^{(0)} \\ \varepsilon_{yy}^{(0)} \\ \gamma_{xy}^{(0)} \end{Bmatrix} + z \begin{Bmatrix} \varepsilon_{xx}^{(1)} \\ \varepsilon_{yy}^{(1)} \\ \gamma_{xy}^{(1)} \end{Bmatrix} + z^3 \begin{Bmatrix} \varepsilon_{xx}^{(3)} \\ \varepsilon_{yy}^{(3)} \\ \gamma_{xy}^{(3)} \end{Bmatrix} \right] dz$$

$$= \int_{-h/2}^{h/2} [c_{ij}] \begin{Bmatrix} \varepsilon_{xx}^{(0)} \\ \varepsilon_{yy}^{(0)} \\ \gamma_{xy}^{(0)} \end{Bmatrix} dz + \int_{-h/2}^{h/2} [c_{ij}] \begin{Bmatrix} \varepsilon_{xx}^{(1)} \\ \varepsilon_{yy}^{(1)} \\ \gamma_{xy}^{(1)} \end{Bmatrix} zdz + \int_{-h/2}^{h/2} [c_{ij}] \begin{Bmatrix} \varepsilon_{xx}^{(3)} \\ \varepsilon_{yy}^{(3)} \\ \gamma_{xy}^{(3)} \end{Bmatrix} z^3 dz$$

$$= [A_{ij}]\{\varepsilon^{(0)}\} + [B_{ij}]\{\varepsilon^{(1)}\} + [E_{ij}]\{\varepsilon^{(3)}\}$$

Moments,

$$\begin{bmatrix} M_x \\ M_y \\ M_{xy} \end{bmatrix} = \int_{-h/2}^{h/2} \begin{bmatrix} \sigma_x \\ \sigma_y \\ \sigma_{xy} \end{bmatrix} z\ dz$$

$$= \int_{-h/2}^{h/2} [c_{ij}] \begin{Bmatrix} \varepsilon_{xx} \\ \varepsilon_{yy} \\ \gamma_{xy} \end{Bmatrix} zdz \quad for\ i,j = 1,2,3$$

$$= \int_{-h/2}^{h/2} [c_{ij}] \left[\begin{Bmatrix} \varepsilon_{xx}^{(0)} \\ \varepsilon_{yy}^{(0)} \\ \gamma_{xy}^{(0)} \end{Bmatrix} + z \begin{Bmatrix} \varepsilon_{xx}^{(1)} \\ \varepsilon_{yy}^{(1)} \\ \gamma_{xy}^{(1)} \end{Bmatrix} + z^3 \begin{Bmatrix} \varepsilon_{xx}^{(3)} \\ \varepsilon_{yy}^{(3)} \\ \gamma_{xy}^{(3)} \end{Bmatrix} \right] zdz$$

$$= \int_{-h/2}^{h/2} [c_{ij}] \begin{Bmatrix} \varepsilon_{xx}^{(0)} \\ \varepsilon_{yy}^{(0)} \\ \gamma_{xy}^{(0)} \end{Bmatrix} zdz + \int_{-h/2}^{h/2} [c_{ij}] \begin{Bmatrix} \varepsilon_{xx}^{(1)} \\ \varepsilon_{yy}^{(1)} \\ \gamma_{xy}^{(1)} \end{Bmatrix} z^2 dz + \int_{-h/2}^{h/2} [c_{ij}] \begin{Bmatrix} \varepsilon_{xx}^{(3)} \\ \varepsilon_{yy}^{(3)} \\ \gamma_{xy}^{(3)} \end{Bmatrix} z^4 dz$$

$$= [B_{ij}]\{\varepsilon^{(0)}\} + [D_{ij}]\{\varepsilon^{(1)}\} + [F_{ij}]\{\varepsilon^{(3)}\}$$

Transverse shear forces,

$$\begin{bmatrix} Q_x \\ Q_y \end{bmatrix} = \int\limits_{-h/2}^{h/2} \begin{bmatrix} \sigma_{xz} \\ \sigma_{yz} \end{bmatrix} dz$$

$$= \int\limits_{-h/2}^{h/2} [c_{ij}] \begin{Bmatrix} \gamma_{xz} \\ \gamma_{yz} \end{Bmatrix} dz \qquad for\ i,j = 4,5$$

$$= \int\limits_{-h/2}^{h/2} [c_{ij}] \left[\begin{Bmatrix} \gamma_{xz}^{(0)} \\ \gamma_{yz}^{(0)} \end{Bmatrix} + z^2 \begin{Bmatrix} \gamma_{xz}^{(2)} \\ \gamma_{yz}^{(2)} \end{Bmatrix} \right] dz$$

$$= \int\limits_{-h/2}^{h/2} [c_{ij}] \begin{Bmatrix} \gamma_{xz}^{(0)} \\ \gamma_{yz}^{(0)} \end{Bmatrix} dz + \int\limits_{-h/2}^{h/2} [c_{ij}] \begin{Bmatrix} \gamma_{xz}^{(2)} \\ \gamma_{yz}^{(2)} \end{Bmatrix} z^2 dz$$

$$= [A_{ij}]\{\gamma^{(0)}\} + [D_{ij}]\{\gamma^{(2)}\}$$

Higher order in plane stress resultants:

$$\begin{bmatrix} P_x \\ P_y \\ P_{xy} \end{bmatrix} = \int_{-h/2}^{h/2} \begin{bmatrix} \sigma_x \\ \sigma_y \\ \sigma_{xy} \end{bmatrix} z^3 dz$$

$$= \int_{-h/2}^{h/2} [c_{ij}] \begin{Bmatrix} \varepsilon_{xx} \\ \varepsilon_{yy} \\ \gamma_{xy} \end{Bmatrix} z^3 dz \quad for\ i,j = 1,2,3$$

$$= \int_{-h/2}^{h/2} [c_{ij}] \left[\begin{Bmatrix} \varepsilon_{xx}^{(0)} \\ \varepsilon_{yy}^{(0)} \\ \gamma_{xy}^{(0)} \end{Bmatrix} + z \begin{Bmatrix} \varepsilon_{xx}^{(1)} \\ \varepsilon_{yy}^{(1)} \\ \gamma_{xy}^{(1)} \end{Bmatrix} + z^3 \begin{Bmatrix} \varepsilon_{xx}^{(3)} \\ \varepsilon_{yy}^{(3)} \\ \gamma_{xy}^{(3)} \end{Bmatrix} \right] z^3 dz$$

$$= \int\limits_{-h/2}^{h/2} [c_{ij}] \begin{Bmatrix} \varepsilon_{xx}^{(0)} \\ \varepsilon_{yy}^{(0)} \\ \gamma_{xy}^{(0)} \end{Bmatrix} z^3 dz + \int\limits_{-h/2}^{h/2} [c_{ij}] \begin{Bmatrix} \varepsilon_{xx}^{(1)} \\ \varepsilon_{yy}^{(1)} \\ \gamma_{xy}^{(1)} \end{Bmatrix} z^4 dz + \int\limits_{-h/2}^{h/2} [c_{ij}] \begin{Bmatrix} \varepsilon_{xx}^{(3)} \\ \varepsilon_{yy}^{(3)} \\ \gamma_{xy}^{(3)} \end{Bmatrix} z^6 dz$$

$$= [E_{ij}]\{\varepsilon^{(0)}\} + [F_{ij}]\{\varepsilon^{(1)}\} + [H_{ij}]\{\varepsilon^{(3)}\}$$

Higher order transverse stress resultants:

$$\begin{bmatrix} R_x \\ R_y \end{bmatrix} = \int\limits_{-h/2}^{h/2} \begin{bmatrix} \sigma_{xz} \\ \sigma_{yz} \end{bmatrix} z^2 dz$$

$$= \int\limits_{-h/2}^{h/2} [c_{ij}] \begin{Bmatrix} \gamma_{xz} \\ \gamma_{yz} \end{Bmatrix} dz \qquad for\ i,j = 4,5$$

$$= \int\limits_{-h/2}^{h/2} [c_{ij}] \left[\begin{Bmatrix} \gamma_{xz}^{(0)} \\ \gamma_{yz}^{(0)} \end{Bmatrix} + z^2 \begin{Bmatrix} \gamma_{xz}^{(2)} \\ \gamma_{yz}^{(2)} \end{Bmatrix} \right] z^2 dz$$

$$= \int_{-h/2}^{h/2} [c_{ij}] \begin{Bmatrix} \gamma_{xz}^{(0)} \\ \gamma_{yz}^{(0)} \end{Bmatrix} z^2 dz + \int_{-h/2}^{h/2} [c_{ij}] \begin{Bmatrix} \gamma_{xz}^{(2)} \\ \gamma_{yz}^{(2)} \end{Bmatrix} z^4 dz$$

$$= [D_{ij}]\{\gamma^{(0)}\} + [F_{ij}]\{\gamma^{(2)}\}$$

Here the higher order in plane and transverse stress resultants P_x, P_y, P_{xy} and R_x, R_y have emerged due to higher order shear deformation theory but have no physical sense regarding their nature.

Internal forces per unit length of the plate is written in matrix form as

$$
\begin{Bmatrix} N_x \\ N_y \\ N_{xy} \\ M_x \\ M_y \\ M_{xy} \\ P_x \\ P_y \\ P_{xy} \\ Q_y \\ Q_x \\ R_y \\ R_x \end{Bmatrix} =
\begin{bmatrix}
A_{11} & A_{12} & A_{13} & B_{11} & B_{12} & B_{13} & E_{11} & E_{12} & E_{13} & 0 & 0 & 0 & 0 \\
A_{12} & A_{22} & A_{23} & B_{12} & B_{22} & B_{23} & E_{12} & E_{22} & E_{23} & 0 & 0 & 0 & 0 \\
A_{13} & A_{23} & A_{33} & B_{13} & B_{23} & B_{33} & E_{13} & E_{23} & E_{33} & 0 & 0 & 0 & 0 \\
B_{11} & B_{12} & B_{13} & D_{11} & D_{12} & D_{13} & F_{11} & F_{12} & F_{13} & 0 & 0 & 0 & 0 \\
B_{12} & B_{22} & B_{23} & D_{12} & D_{22} & D_{23} & F_{12} & F_{22} & F_{23} & 0 & 0 & 0 & 0 \\
B_{13} & B_{23} & B_{33} & D_{13} & D_{23} & D_{33} & F_{13} & F_{23} & F_{33} & 0 & 0 & 0 & 0 \\
E_{11} & E_{12} & E_{13} & F_{11} & F_{12} & F_{13} & H_{11} & H_{12} & H_{13} & 0 & 0 & 0 & 0 \\
E_{12} & E_{22} & E_{23} & F_{12} & F_{22} & F_{23} & H_{12} & H_{22} & H_{23} & 0 & 0 & 0 & 0 \\
E_{13} & E_{23} & E_{33} & F_{13} & F_{23} & F_{33} & H_{13} & H_{23} & H_{33} & 0 & 0 & 0 & 0 \\
0 & 0 & 0 & 0 & 0 & 0 & 0 & 0 & 0 & A_{44} & A_{45} & D_{44} & D_{45} \\
0 & 0 & 0 & 0 & 0 & 0 & 0 & 0 & 0 & A_{45} & A_{55} & D_{45} & D_{55} \\
0 & 0 & 0 & 0 & 0 & 0 & 0 & 0 & 0 & D_{44} & D_{45} & F_{44} & F_{45} \\
0 & 0 & 0 & 0 & 0 & 0 & 0 & 0 & 0 & D_{45} & D_{55} & F_{45} & F_{55}
\end{bmatrix}
\begin{Bmatrix} \varepsilon_{xx}^{(0)} \\ \varepsilon_{yy}^{(0)} \\ \gamma_{xy}^{(0)} \\ \varepsilon_{xx}^{(1)} \\ \varepsilon_{yy}^{(1)} \\ \gamma_{xy}^{(1)} \\ \varepsilon_{xx}^{(3)} \\ \varepsilon_{yy}^{(3)} \\ \gamma_{xy}^{(3)} \\ \gamma_{yz}^{(0)} \\ \gamma_{xz}^{(0)} \\ \gamma_{yz}^{(2)} \\ \gamma_{xz}^{(2)} \end{Bmatrix}
$$

$$
[D] =
\begin{bmatrix}
A_{11} & A_{12} & A_{13} & B_{11} & B_{12} & B_{13} & E_{11} & E_{12} & E_{13} & 0 & 0 & 0 & 0 \\
A_{12} & A_{22} & A_{23} & B_{12} & B_{22} & B_{23} & E_{12} & E_{22} & E_{23} & 0 & 0 & 0 & 0 \\
A_{13} & A_{23} & A_{33} & B_{13} & B_{23} & B_{33} & E_{13} & E_{23} & E_{33} & 0 & 0 & 0 & 0 \\
B_{11} & B_{12} & B_{13} & D_{11} & D_{12} & D_{13} & F_{11} & F_{12} & F_{13} & 0 & 0 & 0 & 0 \\
B_{12} & B_{22} & B_{23} & D_{12} & D_{22} & D_{23} & F_{12} & F_{22} & F_{23} & 0 & 0 & 0 & 0 \\
B_{13} & B_{23} & B_{33} & D_{13} & D_{23} & D_{33} & F_{13} & F_{23} & F_{33} & 0 & 0 & 0 & 0 \\
E_{11} & E_{12} & E_{13} & F_{11} & F_{12} & F_{13} & H_{11} & H_{12} & H_{13} & 0 & 0 & 0 & 0 \\
E_{12} & E_{22} & E_{23} & F_{12} & F_{22} & F_{23} & H_{12} & H_{22} & H_{23} & 0 & 0 & 0 & 0 \\
E_{13} & E_{23} & E_{33} & F_{13} & F_{23} & F_{33} & H_{13} & H_{23} & H_{33} & 0 & 0 & 0 & 0 \\
0 & 0 & 0 & 0 & 0 & 0 & 0 & 0 & 0 & A_{44} & A_{45} & D_{44} & D_{45} \\
0 & 0 & 0 & 0 & 0 & 0 & 0 & 0 & 0 & A_{45} & A_{55} & D_{45} & D_{55} \\
0 & 0 & 0 & 0 & 0 & 0 & 0 & 0 & 0 & D_{44} & D_{45} & F_{44} & F_{45} \\
0 & 0 & 0 & 0 & 0 & 0 & 0 & 0 & 0 & D_{45} & D_{55} & F_{45} & F_{55}
\end{bmatrix}
$$

Where D is the constitutive relation matrix

A_{ij} denotes extensional stiffnesses, D_{ij} denotes bending stiffnesses. B_{ij} the bending extensional coupling stiffnesses and E_{ij}, F_{ij}, H_{ij} are the higher order stiffnesses

$$\left(A_{ij}, B_{ij}, D_{ij}, E_{ij}, F_{ij}, H_{ij}\right) = \int_{-h/2}^{h/2} c'_{ij} \, (1, z, z^2, z^3, z^4, z^6) dz$$

The stiffnesses A_{ij}, D_{ij}, F_{ij} are defined for i,j=1,2,3 and for i,j=4,5 where as $B_{ij}, E_{ij} H_{ij}$ are valid for i,j=1,2,3

$$A_{11} = \int_{-h/2}^{h/2} \frac{E(z)}{1 - v_1 v_2} dz$$

Where $E(z) = (E_c - E_m)\left(\frac{z}{h} + \frac{1}{2}\right)^k + E_m$; E_C is the Young's modulus of ceramic ; E_m is the Young's modulus of metal and v_1 and v_2 are the poisson's ratio of metal and ceramic respectively.
Therefore,

$$A_{11} = \frac{1}{1 - v_1 v_2} \int_{-h/2}^{h/2} \left[(E_c - E_m)\left(\frac{z}{h} + \frac{1}{2}\right)^k + E_m\right]$$

$$= \frac{h}{1 - v_1 v_2} \left[\frac{(E_c - E_m)}{k + 1} + E_m\right]$$

$$A_{12} = \int_{-h/2}^{h/2} \frac{v_1 E(z)}{1 - v_1 v_2} dz$$

$$= \frac{v_1}{1 - v_1 v_2} \int_{-h/2}^{h/2} \left[(E_c - E_m)\left(\frac{z}{h} + \frac{1}{2}\right)^k + E_m\right] dz$$

$$= \frac{h v_1}{1 - v_1 v_2} \left[\frac{(E_c - E_m)}{k + 1} + E_m\right]$$

$A_{22} = A_{11}$

$$A_{13} = A_{23} = 0$$

$$A_{33} = \int_{-h/2}^{h/2} \frac{E(z)}{2(1 + v_1)} dz$$

$$= \frac{1}{2(1+v_1)} \int_{-h/2}^{h/2} \left[(E_c - E_m)\left(\frac{z}{h}+\frac{1}{2}\right)^k + E_m \right] dz$$

$$= \frac{1}{2(1+v_1)} \left[\frac{(E_c - E_m)}{k+1} + E_m \right]$$

$$B_{11} = \int_{-h/2}^{h/2} \frac{E(z)}{1-v_1v_2} z\,dz$$

$$= \frac{1}{1-v_1v_2} \int_{-h/2}^{h/2} \left[(E_c - E_m)\left(\frac{z}{h}+\frac{1}{2}\right)^k + E_m \right] dz$$

$$= \frac{h^2}{1-v_1v_2} \left[\frac{(E_c - E_m)}{k+2} - \frac{(E_c - E_m)}{2(k+1)} \right]$$

$$B_{22} = B_{11}$$

$$B_{12} = \int_{-h/2}^{h/2} \frac{v_1 E(z)}{1-v_1v_2} z\,dz$$

$$= \frac{v_1}{1-v_1v_2} \int_{-h/2}^{h/2} \left[(E_c - E_m)\left(\frac{z}{h}+\frac{1}{2}\right)^k + E_m \right] z\,dz$$

$$= \frac{v_1 h^2}{1-v_1v_2} \left[\frac{(E_c - E_m)}{k+2} - \frac{(E_c - E_m)}{2(k+1)} \right]$$

$$B_{13} = B_{23} = 0$$

$$B_{33} = \int_{-h/2}^{h/2} \frac{E(z)}{2(1+v_1)} z\,dz$$

$$= \frac{1}{2(1+v_1)} \int_{-h/2}^{h/2} \left[(E_c - E_m)\left(\frac{z}{h}+\frac{1}{2}\right)^k + E_m \right] z\,dz$$

$$= \frac{h^2}{2(1+v_1)} \left[\frac{(E_c - E_m)}{k+2} - \frac{(E_c - E_m)}{2(k+1)} \right]$$

$$D_{11} = \int\limits_{-h/2}^{h/2} \frac{E(z)}{1 - \nu_1\nu_2} z^2 \, dz$$

$$= \frac{1}{1 - \nu_1\nu_2} \int\limits_{-h/2}^{h/2} \left[(E_c - E_m)\left(\frac{z}{h} + \frac{1}{2}\right)^k + E_m \right] z^2 dz$$

$$= \frac{h^3}{(1 - \nu_1\nu_2)} \left[\frac{(E_c - E_m)}{k + 3} - \frac{(E_c - E_m)}{(k + 2)} + \frac{(E_c - E_m)}{4(k + 1)} + \frac{E_m}{12} \right]$$

$D_{22} = D_{11}$

$D_{13} = D_{23} = 0$

$$D_{12} = \int\limits_{-h/2}^{h/2} \frac{\nu_1 E(z)}{1 - \nu_1\nu_2} z^2 dz$$

$$= \frac{\nu_1}{1 - \nu_1\nu_2} \int\limits_{-h/2}^{h/2} \left[(E_c - E_m)\left(\frac{z}{h} + \frac{1}{2}\right)^k + E_m \right] z^2 dz$$

$$= \frac{\nu_1 h^3}{1 - \nu_1\nu_2} \left[\frac{(E_c - E_m)}{k + 3} - \frac{(E_c - E_m)}{(k + 2)} + \frac{(E_c - E_m)}{4(k + 1)} + \frac{E_m}{12} \right]$$

$$D_{33} = \int\limits_{-h/2}^{h/2} \frac{E(z)}{2(1 + \nu_1)} z^2 dz$$

$$= \frac{1}{2(1 + \nu_1)} \int\limits_{-h/2}^{h/2} \left[(E_c - E_m)\left(\frac{z}{h} + \frac{1}{2}\right)^k + E_m \right] z^2 dz$$

$$= \frac{h^3}{2(1 + \nu_1)} \left[\frac{(E_c - E_m)}{k + 3} - \frac{(E_c - E_m)}{(k + 2)} + \frac{(E_c - E_m)}{4(k + 1)} + \frac{E_m}{12} \right]$$

Computing higher order stiffness terms $E_{ij}, F_{ij}, and\ H_{ij}$

$$E_{11} = \int\limits_{-h/2}^{h/2} \frac{E(z)}{1 - \nu_1\nu_2} z^3 \, dz$$

$$= \frac{1}{1 - \nu_1 \nu_2} \int\limits_{-h/2}^{h/2} \left[(E_c - E_m) \left(\frac{z}{h} + \frac{1}{2} \right)^k + E_m \right] z^3 dz$$

$$= \frac{h^4}{8(1 - \nu_1 \nu_2)} \left[\frac{8(E_c - E_m)}{k + 4} - \frac{12(E_c - E_m)}{(k + 3)} + \frac{6(E_c - E_m)}{(k + 2)} - \frac{(E_c - E_m)}{k + 1} \right]$$

$$E_{12} = \int\limits_{-h/2}^{h/2} \frac{\nu_1 E(z)}{1 - \nu_1 \nu_2} z^3 dz$$

$$= \frac{\nu_1}{1 - \nu_1 \nu_2} \int\limits_{-h/2}^{h/2} \left[(E_c - E_m) \left(\frac{z}{h} + \frac{1}{2} \right)^k + E_m \right] z^3 dz$$

$$= \frac{\nu_1 h^4}{8(1 - \nu_1 \nu_2)} \left[\frac{8(E_c - E_m)}{k + 4} - \frac{12(E_c - E_m)}{(k + 3)} + \frac{6(E_c - E_m)}{(k + 2)} - \frac{(E_c - E_m)}{k + 1} \right]$$

$$E_{22} = E_{11}$$

$$E_{13} = E_{23} = 0$$

$$E_{33} = \int\limits_{-h/2}^{h/2} \frac{E(z)}{2(1 + \nu_1)} z^3 dz$$

$$= \frac{1}{2(1 + \nu_1)} \int\limits_{-h/2}^{h/2} \left[(E_c - E_m) \left(\frac{z}{h} + \frac{1}{2} \right)^k + E_m \right] z^3 dz$$

$$= \frac{h^4}{16(1 + \nu_1)} \left[\frac{8(E_c - E_m)}{k + 4} - \frac{12(E_c - E_m)}{(k + 3)} + \frac{6(E_c - E_m)}{(k + 2)} - \frac{(E_c - E_m)}{k + 1} \right]$$

$$F_{11} = \int\limits_{-h/2}^{h/2} \frac{E(z)}{1 - \nu_1 \nu_2} z^4 dz$$

$$= \frac{1}{1 - \nu_1\nu_2} \int_{-h/2}^{h/2} \left[(E_c - E_m)\left(\frac{z}{h} + \frac{1}{2}\right)^k + E_m \right] z^4 dz$$

$$= \frac{h^5}{(1 - \nu_1\nu_2)} \left[\frac{(E_c - E_m)}{k + 5} - \frac{2(E_c - E_m)}{(k + 4)} + \frac{3(E_c - E_m)}{2(k + 3)} - \frac{(E_c - E_m)}{2(k + 2)} + \frac{(E_c - E_m)}{16(k + 1)} + \frac{E_m}{80} \right]$$

$$F_{12} = \int_{-h/2}^{h/2} \frac{\nu_1 E(z)}{1 - \nu_1\nu_2} z^4 dz$$

$$= \frac{\nu_1}{1 - \nu_1\nu_2} \int_{-h/2}^{h/2} \left[(E_c - E_m)\left(\frac{z}{h} + \frac{1}{2}\right)^k + E_m \right] z^4 dz$$

$$= \frac{\nu_1 h^5}{(1 - \nu_1\nu_2)} \left[\frac{(E_c - E_m)}{k + 5} - \frac{2(E_c - E_m)}{(k + 4)} + \frac{3(E_c - E_m)}{2(k + 3)} - \frac{(E_c - E_m)}{2(k + 2)} + \frac{(E_c - E_m)}{16(k + 1)} + \frac{E_m}{80} \right]$$

$$F_{22} = F_{11}$$

$$F_{13} = F_{23} = 0$$

$$F_{33} = \int_{-h/2}^{h/2} \frac{E(z)}{2(1 + \nu_1)} z^4 dz$$

$$= \frac{1}{2(1 + \nu_1)} \int_{-h/2}^{h/2} \left[(E_c - E_m)\left(\frac{z}{h} + \frac{1}{2}\right)^k + E_m \right] z^4 dz$$

$$= \frac{h^5}{2(1 + \nu_1)} \left[\frac{(E_c - E_m)}{k + 5} - \frac{2(E_c - E_m)}{(k + 4)} + \frac{3(E_c - E_m)}{2(k + 3)} - \frac{(E_c - E_m)}{2(k + 2)} + \frac{(E_c - E_m)}{16(k + 1)} + \frac{E_m}{80} \right]$$

$$H_{11} = \int_{-h/2}^{h/2} \frac{E(z)}{1 - \nu_1\nu_2} z^6 dz$$

$$= \frac{1}{1 - \nu_1\nu_2} \int_{-h/2}^{h/2} \left[(E_c - E_m)\left(\frac{z}{h} + \frac{1}{2}\right)^k + E_m \right] z^6 dz$$

$$= \frac{h^7}{(1 - \nu_1\nu_2)} \left[\frac{(E_c - E_m)}{k+7} - \frac{3(E_c - E_m)}{(k+6)} + \frac{15(E_c - E_m)}{4(k+5)} - \frac{5(E_c - E_m)}{2(k+4)} + \frac{5(E_c - E_m)}{16(k+3)} \right.$$
$$\left. - \frac{3(E_c - E_m)}{16(k+2)} + \frac{(E_c - E_m)}{64(k+1)} + \frac{E_m}{448} \right]$$

$$H_{12} = \int_{-h/2}^{h/2} \frac{\nu_1 E(z)}{1 - \nu_1\nu_2} z^6 dz$$

$$= \frac{\nu_1}{1 - \nu_1\nu_2} \int_{-h/2}^{h/2} \left[(E_c - E_m)\left(\frac{z}{h} + \frac{1}{2}\right)^k + E_m \right] z^6 dz$$

$$= \frac{\nu_1 h^7}{(1 - \nu_1\nu_2)} \left[\frac{(E_c - E_m)}{k+7} - \frac{3(E_c - E_m)}{(k+6)} + \frac{15(E_c - E_m)}{4(k+5)} - \frac{5(E_c - E_m)}{2(k+4)} + \frac{5(E_c - E_m)}{16(k+3)} \right.$$
$$\left. - \frac{3(E_c - E_m)}{16(k+2)} + \frac{(E_c - E_m)}{64(k+1)} + \frac{E_m}{448} \right]$$

$H_{22} = H_{11}$

$H_{13} = H_{23} = 0$

$$H_{33} = \int_{-h/2}^{h/2} \frac{E(z)}{2(1 + \nu_1)} z^6 dz$$

$$= \frac{1}{2(1 + \nu_1)} \int_{-h/2}^{h/2} \left[(E_c - E_m)\left(\frac{z}{h} + \frac{1}{2}\right)^k + E_m \right] z^6 dz$$

$$= \frac{h^7}{2(1 + \nu_1)} \left[\frac{(E_c - E_m)}{k+7} - \frac{3(E_c - E_m)}{(k+6)} + \frac{15(E_c - E_m)}{4(k+5)} - \frac{5(E_c - E_m)}{2(k+4)} + \frac{5(E_c - E_m)}{16(k+3)} \right.$$
$$\left. - \frac{3(E_c - E_m)}{16(k+2)} + \frac{(E_c - E_m)}{64(k+1)} + \frac{E_m}{448} \right]$$

The constitutive elements related to shear stiffnesses are,

$$A_{45} = 0$$

$$A_{44} = A_{55} = \int_{-h/2}^{h/2} \frac{E(z)}{2(1 + \nu_1)} dz$$

$$= \frac{1}{2(1+\nu_1)} \int_{-h/2}^{h/2} \left[(E_c - E_m) \left(\frac{z}{h} + \frac{1}{2} \right)^k + E_m \right] dz$$

$$= \frac{h}{2(1+\nu_1)} \left[\frac{(E_c - E_m)}{k+1} + E_m \right]$$

$$D_{45} = F_{45} = 0$$

$$D_{44} = D_{55} = \int_{-h/2}^{h/2} \frac{E(z)}{2(1+\nu_1)} z^2 dz$$

$$= \frac{1}{2(1+\nu_1)} \int_{-h/2}^{h/2} \left[(E_c - E_m) \left(\frac{z}{h} + \frac{1}{2} \right)^k + E_m \right] z^2 dz$$

$$= \frac{h^3}{2(1+\nu_1)} \left[\frac{(E_c - E_m)}{k+3} - \frac{(E_c - E_m)}{(k+2)} + \frac{(E_c - E_m)}{4(k+1)} + \frac{E_m}{12} \right]$$

$$F_{44} = F_{55} = \int_{-h/2}^{h/2} \frac{E(z)}{2(1+\nu_1)} z^4 dz$$

$$= \frac{1}{2(1+\nu_1)} \int_{-h/2}^{h/2} \left[(E_c - E_m) \left(\frac{z}{h} + \frac{1}{2} \right)^k + E_m \right] z^4 dz$$

$$= \frac{h^5}{2(1+\nu_1)} \left[\frac{(E_c - E_m)}{k+5} - \frac{2(E_c - E_m)}{(k+4)} + \frac{3(E_c - E_m)}{2(k+3)} - \frac{(E_c - E_m)}{2(k+2)} + \frac{(E_c - E_m)}{16(k+1)} + \frac{E_m}{80} \right]$$

3.4.6 Finite Element Formulation of Functionally Graded Plate

The finite element formulation discussed here, is based on the governing equation derived in the preceding section. Here the elastic and geometric stiffness, the mass matrix and the load vector of the element are derived using the Principle of Total Potential Energy. Next, the matrices are transformed and assembled to obtain the system equations. The subspace iteration technique is resorted to find out eigen solution.

3.4.6.1 Isoparametric Element

An eight noded serendipity isoparametric element have been used in the analysis so that both geometry and displacement field are expressed by the same set of shape functions. The parent element in local coordinate system can be mapped to an arbitrary shape in the Cartesian coordinate system.

A flat Mindlin eight noded plate element with seven degrees of freedom (D.O.F) at each node, i.e., u, v, w, θ_x, θ_y, Φ_x and Φ_y is used in the analysis. The co-ordinates and the elastic parameters inside the element can be interpolated using shape function (interpolation function) N_i as given in Figure 2.5.

$$x = \sum_{i=1}^{8} N_i(\xi,\eta)x_i \qquad y = \sum_{i=1}^{8} N_i(\xi,\eta)y_i$$

where x_i and y_i are the global co-ordinates at a node i.

$$u_0 = \sum_{i=1}^{8} N_i(\xi,\eta)u_{o_i} \quad v_0 = \sum_{i=1}^{8} N_i(\xi,\eta)v_{o_i} \quad w = \sum_{i=1}^{8} N_i(\xi,\eta)w_i$$

$$\theta_x = \sum_{i=1}^{8} N_i(\xi,\eta)\theta_{x_i} \quad \theta_y = \sum_{i=1}^{8} N_i(\xi,\eta)\theta_{y_i} \quad \Phi_x = \sum_{i=1}^{8} N_i(\xi,\eta)\Phi_{x_i} \quad \Phi_y = \sum_{i=1}^{8} N_i(\xi,\eta)\Phi_{y_i}$$

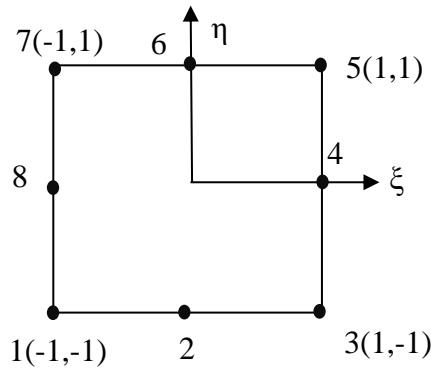**Fig 3.4.6.1.a:** 8 Noded Serendipity element

The shape functions N_i are defined as

$N_i = (1+\xi\xi_i) (1+\eta\eta_i)(\xi\xi_i +\eta\eta_i -1)/4 \;; i = 1, 3, 5, 7$

$N_i = (1-\xi^2) (1+\eta\eta_i)/2 \;; i = 2,6$

$N_i = (1-\eta^2) (1+\xi\xi_i) /2 \;; i = 4,8$

Where ξ and η are the local natural co-ordinates of the element and ξ_i and η_i are the value of them at node i.

The strains at the mid-plane of the plate are given by,

$$
\begin{bmatrix}
\varepsilon_{xx}^{(0)} \\
\varepsilon_{yy}^{(0)} \\
\gamma_{xy}^{(0)} \\
\varepsilon_{xx}^{(1)} \\
\varepsilon_{yy}^{(1)} \\
\gamma_{xy}^{(1)} \\
\varepsilon_{xx}^{(3)} \\
\varepsilon_{yy}^{(3)} \\
\gamma_{xy}^{(3)} \\
\gamma_{yz}^{(0)} \\
\gamma_{xz}^{(0)} \\
\gamma_{yz}^{(2)} \\
\gamma_{xz}^{(2)}
\end{bmatrix}
= \sum_{j=1}^{8}
\begin{bmatrix}
N_{i,x} & 0 & 0 & 0 & 0 & 0 & 0 \\
0 & N_{i,y} & 0 & 0 & 0 & 0 & 0 \\
N_{i,y} & N_{i,x} & 0 & 0 & 0 & 0 & 0 \\
0 & 0 & 0 & 0 & 0 & 0 & N_{i,x} \\
0 & 0 & 0 & 0 & 0 & N_{i,y} & 0 \\
0 & 0 & 0 & 0 & 0 & N_{i,x} & N_{i,y} \\
0 & 0 & 0 & 0 & -c_1 N_{i,x} & 0 & -c_1 N_{i,x} \\
0 & 0 & 0 & -c_1 N_{i,y} & 0 & -c_1 N_{i,y} & 0 \\
0 & 0 & 0 & -c_1 N_{i,x} & -c_1 N_{i,y} & -c_1 N_{i,x} & -c_1 N_{i,y} \\
0 & 0 & N_{i,y} & 0 & 0 & N_i & 0 \\
0 & 0 & N_{i,x} & 0 & 0 & 0 & N_i \\
0 & 0 & 0 & -c_2 N_i & 0 & -c_2 N_i & 0 \\
0 & 0 & 0 & 0 & -c_2 N_i & 0 & -c_2 N_i
\end{bmatrix}
\begin{bmatrix}
u_{0j} \\
v_{0j} \\
w_{0j} \\
\theta_{yj} \\
\theta_{xj} \\
\Phi_{yj} \\
\Phi_{xj}
\end{bmatrix}
$$

Or, $\{\varepsilon\} = [B]\{d\}$, where, $[B]$ is the linear strain- displacement matrix where $c_1 = \dfrac{4}{3h^2}$ and $c_2 = 3c_1$ and $\{d\}$ is the nodal displacement matrix

3.4.6.2 Inertia matrix
Kinetic energy of any vibrating FGM plate for small displacement:

$$
T = \frac{1}{2}\int \rho(z)\dot{u}'\dot{u} \dots\dots\dots\dots (i) \ \ where\ \rho(z) = (\rho_c - \rho_m)\left(\frac{z}{h} + \frac{1}{2}\right)^k + \rho_m
$$

$$
u = \begin{bmatrix} u \\ v \\ w \end{bmatrix} = \begin{bmatrix} u_0(x,y,t) + z\Phi_x(x,y,t) + c_1 z^3\left(\Phi_x + w_{0,x}\right) \\ v_0(x,y,t) + z\phi_y(x,y,t) + c_1 z^3\left(\Phi_y + w_{0,y}\right) \\ w_0 \end{bmatrix}
$$

$$
= \begin{bmatrix}
1 & 0 & 0 & z - c_2 z^3 & 0 & -c_2 z^3 & 0 \\
0 & 1 & 0 & 0 & z - c_2 z^3 & 0 & -c_2 z^3 \\
0 & 0 & 1 & 0 & 0 & 0 & 0
\end{bmatrix}
\begin{Bmatrix}
u_0 \\
v_0 \\
w_0 \\
\Phi_x \\
\Phi_y \\
\theta_x \\
\theta_y
\end{Bmatrix}
$$

$$
= [N]\{d\} \quad where\ c_2 = \frac{4}{3h^2}
$$

35

If $\{d\} = \begin{Bmatrix} u_0 \\ v_0 \\ w_0 \\ \theta_y \\ \theta_x \\ \phi_y \\ \phi_x \end{Bmatrix}$; then $[N] = \begin{bmatrix} 1 & 0 & 0 & 0 & -c_2z^3 & 0 & z-c_2z^3 \\ 0 & 1 & 0 & -c_2z^3 & 0 & z-c_2z^3 & 0 \\ 0 & 0 & 1 & 0 & 0 & 0 & 0 \end{bmatrix}$

Therefore $\{u\} = \begin{bmatrix} 1 & 0 & 0 & 0 & -c_2z^3 & 0 & z-c_2z^3 \\ 0 & 1 & 0 & -c_2z^3 & 0 & z-c_2z^3 & 0 \\ 0 & 0 & 1 & 0 & 0 & 0 & 0 \end{bmatrix} \begin{Bmatrix} u_0 \\ v_0 \\ w_0 \\ \theta_y \\ \theta_x \\ \phi_y \\ \phi_x \end{Bmatrix}$

$=[N]\{d\}$written by rearranging elements of $\{d\}$ matrix

From equation (i)

$$T = \frac{1}{2}\left(\int \rho(z)\{\dot{d}\}'\{N\}'\{N\}\{\dot{d}\}dz\right)dA$$

$$= \frac{1}{2}\int \{\dot{d}\}'[m]\{\dot{d}\}$$

Where $[m] = \{N\}'\rho(z)\{N\}$ $\quad$ *is the inertia matrix*

Therefore $[m] = \begin{bmatrix} p & 0 & 0 & 0 & q_2 & 0 & q_1 \\ 0 & p & 0 & q_2 & 0 & q_1 & 0 \\ 0 & 0 & p & 0 & 0 & 0 & 0 \\ 0 & q_2 & 0 & I_2 & 0 & I_3 & 0 \\ q_2 & 0 & 0 & 0 & I_2 & 0 & I_3 \\ 0 & q_1 & 0 & I_3 & 0 & I_1 & 0 \\ q_1 & 0 & 0 & 0 & I_3 & 0 & I_1 \end{bmatrix}$

Where

$$p = \int_{-h/2}^{h/2} \rho(z)dz$$

$$= \int_{-h/2}^{h/2} \left[(\rho_c - \rho_m)\left(\frac{z}{h} + \frac{1}{2}\right)^k + \rho_m\right]dz$$

36

$$= h \left[\frac{(\rho_c - \rho_m)}{k+1} + \rho_m \right]$$

$$q_1 = \int_{-h/2}^{h/2} \rho(z)[z - c_2 z^3]dz \quad where\ c_2 = \frac{4}{3h^2}$$

$$= \int_{-h/2}^{h/2} \rho(z)z\,dz - c_2 \int_{-h/2}^{h/2} \rho(z)z^3 dz$$

$$= \int_{-h/2}^{h/2} \left[(\rho_c - \rho_m)\left(\frac{z}{h}+\frac{1}{2}\right)^k + \rho_m \right] z\,dz - c_2 \int_{-h/2}^{h/2} \left[(\rho_c - \rho_m)\left(\frac{z}{h}+\frac{1}{2}\right)^k + \rho_m \right] z^3 dz$$

$$= h^2 \left[\frac{(\rho_c - \rho_m)}{k+2} - \frac{(\rho_c - \rho_m)}{2(k+1)} \right]$$

$$- c_2 \frac{h^4}{8} \left[\frac{8(\rho_c - \rho_m)}{k+4} - \frac{12(\rho_c - \rho_m)}{(k+3)} + \frac{6(\rho_c - \rho_m)}{(k+2)} - \frac{(\rho_c - \rho_m)}{k+1} \right]$$

$$q_2 = (-c_2) \int_{-h/2}^{h/2} \rho(z)z^3 dz$$

$$= -c_2 \int_{-h/2}^{h/2} \left[(\rho_c - \rho_m)\left(\frac{z}{h}+\frac{1}{2}\right)^k + \rho_m \right] z^3 dz$$

$$= -c_2 \frac{h^4}{8} \left[\frac{8(\rho_c - \rho_m)}{k+4} - \frac{12(\rho_c - \rho_m)}{(k+3)} + \frac{6(\rho_c - \rho_m)}{(k+2)} - \frac{(\rho_c - \rho_m)}{k+1} \right]$$

$$I_1 = \int_{-h/2}^{h/2} \rho(z)\{z - c_2 z^3\}^2 dz$$

$$= \int_{-h/2}^{h/2} \rho(z)z^2 dz - 2c_2 \int_{-h/2}^{h/2} \rho(z)z^4 dz + c_2^2 \int_{-h/2}^{h/2} \rho(z)z^6 dz$$

$$= \int_{-h/2}^{h/2} \left[(\rho_c - \rho_m) \left(\frac{z}{h} + \frac{1}{2} \right)^k + \rho_m \right] z^2 dz$$

$$- 2c_2 \int_{-h/2}^{h/2} \left[(\rho_c - \rho_m) \left(\frac{z}{h} + \frac{1}{2} \right)^k + \rho_m \right] z^4 dz$$

$$+ c_2^2 \int_{-h/2}^{h/2} \left[(\rho_c - \rho_m) \left(\frac{z}{h} + \frac{1}{2} \right)^k + \rho_m \right] z^6 dz$$

$$= \frac{h^4}{8} \left[\frac{8(\rho_c - \rho_m)}{k+4} - \frac{12(\rho_c - \rho_m)}{(k+3)} + \frac{6(\rho_c - \rho_m)}{(k+2)} - \frac{(\rho_c - \rho_m)}{k+1} \right]$$

$$- 2 \left\{ \frac{4}{3h^2} \right\} h^5 \left[\frac{(\rho_c - \rho_m)}{k+5} - \frac{2(\rho_c - \rho_m)}{(k+4)} + \frac{3(\rho_c - \rho_m)}{2(k+3)} - \frac{(\rho_c - \rho_m)}{2(k+2)} \right.$$

$$+ \frac{(\rho_c - \rho_m)}{16(k+1)} + \frac{\rho_m}{80} \right]$$

$$+ \left\{ \frac{4}{3h^2} \right\}^2 h^7 \left[\frac{(\rho_c - \rho_m)}{k+7} - \frac{3(\rho_c - \rho_m)}{(k+6)} + \frac{15(\rho_c - \rho_m)}{4(k+5)} - \frac{5(\rho_c - \rho_m)}{2(k+4)} \right.$$

$$+ \frac{5(\rho_c - \rho_m)}{16(k+3)} - \frac{3(\rho_c - \rho_m)}{16(k+2)} + \frac{(\rho_c - \rho_m)}{64(k+1)} + \frac{\rho_m}{448} \right]$$

$$I_2 = c_2^2 \int_{-h/2}^{h/2} \rho(z) z^6 dz$$

$$= c_2^2 \int_{-h/2}^{h/2} \left[(\rho_c - \rho_m) \left(\frac{z}{h} + \frac{1}{2} \right)^k + \rho_m \right] z^6 dz$$

$$= \left\{ \frac{4}{3h^2} \right\}^2 \times h^7 \left[\frac{(\rho_c - \rho_m)}{k+7} - \frac{3(\rho_c - \rho_m)}{(k+6)} + \frac{15(\rho_c - \rho_m)}{4(k+5)} - \frac{5(\rho_c - \rho_m)}{2(k+4)} + \frac{5(\rho_c - \rho_m)}{16(k+3)} \right.$$

$$\left. - \frac{3(\rho_c - \rho_m)}{16(k+2)} + \frac{(\rho_c - \rho_m)}{64(k+1)} + \frac{\rho_m}{448} \right]$$

$$= \frac{16h^3}{9} \left[\frac{(\rho_c - \rho_m)}{k+7} - \frac{3(\rho_c - \rho_m)}{(k+6)} + \frac{15(\rho_c - \rho_m)}{4(k+5)} - \frac{5(\rho_c - \rho_m)}{2(k+4)} + \frac{5(\rho_c - \rho_m)}{16(k+3)} - \frac{3(\rho_c - \rho_m)}{16(k+2)} \right.$$

$$\left. + \frac{(\rho_c - \rho_m)}{64(k+1)} + \frac{\rho_m}{448} \right]$$

$$I_3 = \int_{-h/2}^{h/2} \rho(z)\{-c_2 z^3\}\{z - c_2 z^3\} dz$$

$$= c_2^2 \int\limits_{-h/2}^{h/2} \rho(z)z^6 dz - c_2 \int\limits_{-h/2}^{h/2} \rho(z)z^4 dz$$

$$= c_2^2 \int\limits_{-h/2}^{h/2} \left[(\rho_c - \rho_m)\left(\frac{z}{h} + \frac{1}{2}\right)^k + \rho_m \right] z^6 dz - c_2 \int\limits_{-h/2}^{h/2} \left[(\rho_c - \rho_m)\left(\frac{z}{h} + \frac{1}{2}\right)^k + \rho_m \right] z^4 dz$$

$$= \left\{\frac{4}{3h^2}\right\}^2 \times h^7 \left[\frac{(\rho_c - \rho_m)}{k+7} - \frac{3(\rho_c - \rho_m)}{(k+6)} + \frac{15(\rho_c - \rho_m)}{4(k+5)} - \frac{5(\rho_c - \rho_m)}{2(k+4)} + \frac{5(\rho_c - \rho_m)}{16(k+3)} \right.$$
$$\left. - \frac{3(\rho_c - \rho_m)}{16(k+2)} + \frac{(\rho_c - \rho_m)}{64(k+1)} + \frac{\rho_m}{448} \right] - \left\{\frac{4}{3h^2}\right\}$$
$$\times h^5 \left[\frac{(\rho_c - \rho_m)}{k+5} - \frac{2(\rho_c - \rho_m)}{(k+4)} + \frac{3(\rho_c - \rho_m)}{2(k+3)} - \frac{(\rho_c - \rho_m)}{2(k+2)} + \frac{(\rho_c - \rho_m)}{16(k+1)} + \frac{\rho_m}{80} \right]$$

Chapter 4

4.0 Numerical results and discussion

The finite element formulation described in the earlier section has been used to generate numerical results to study the effect of side-thickness ratio i.e a/h, volume fraction index (k), different FG materials used as surface materials, different support conditions on natural frequencies of the FGM plate. A comparison with other results is shown to validate the MATLAB code developed.

4.1 Validation study

The results of free vibration analysis of FGM plate structure, of length a=1.0m and width b=1.0m, are presented in Table 4. 1.a and the results are compared with Talha and Singh *et.al.*[11]. For analysing the plate, a program has been developed in MATLAB. The FGM plate has stainless steel as metal on one face with properties $E_1=208\times10^9$ MPa, poisson's ratio(v_1)=0.3177 and density(ρ_1)=8166 kg/m^3 while the other face has ceramic Silicon Nitride(Si_3N_4) with $E_2=322\times10^9$, $v_2=0.24$ and $\rho_2=2370$ kg/m^3.The plate is analysed considering 8X8 mesh using the FEM model. Non- dimensional frequency of free vibration for (a/h) ratios of 10 and different k values is tabulated in Table 4.1.a and compared. *h* is the thickness of plate and non-dimensional frequency, $\omega_n=(\omega a^2/h)(\rho/E_2)^{1/2}$. It is observed that our program works well for medium to high a/h ratios.

Table 4.1a: Non dimensional frequencies for (SUS$_3$O$_4$/Si$_3$N$_4$) FGM plates for SSSS and CCCC conditions for a/h =10 and varying volume fraction index (k)

Boundary condition	a/h	Mode	K=0		K=0.5		K=1		Metal	
			Talha and Singh et al. [11]	Present FEM	Talha and Singh et al. [11]	Present FEM	Talha and Singh et al. [11]	Present FEM	Talha and Singh et al. [11]	Present FEM
SSSS	10	1	5.7523	5.7520	3.9701	3.9720	3.4845	3.4890	2.5154	2.4883
		2	14.0336	13.710	9.6890	9.4450	8.4903	8.2780	6.1361	5.9307
		3	14.0354	13.710	9.6906	9.4450	8.4918	8.2780	6.1370	5.9307
		4	21.6188	21.071	14.9404	14.5250	13.0959	12.730	9.4515	9.116
		5	27.1449	25.680	18.7691	17.6990	16.4526	15.501	11.8664	11.1122
CCCC	10	1	10.1599	9.7962	7.0202	6.7557	6.1489	5.9160	4.4410	4.2462
		2	19.9367	18.7197	13.7978	12.9170	12.0812	11.3068	8.7107	8.1393
		3	19.9367	18.7197	13.7978	12.9178	12.0812	11.3068	8.7107	8.1393
		4	28.1367	26.2875	19.4845	18.1453	17.0625	15.8778	12.2919	11.429
		5	34.6017	30.5801	23.9945	21.4498	20.9992	18.7645	15.1084	13.5547

4.2 Mesh convergence study using square plate

FGM plate of square shape and made of Al/Al$_2$O$_3$ as metal and ceramic combination has been studied to check mesh convergence results. Four types of meshes (e.g 2×2, 4×4, 6×6, 8×8) are taken in the study. The properties of metal (Al) are as follows: E_1=70×10^9 MPa, poisson's ratio(ν_1)=0.3 and density(ρ_1)=2707 kg/m^3 while the other face has ceramic Alumina(Al$_2$O$_3$) with E_2=380×10^9 N/m^2, ν_2= 0.3 and ρ_2= 3800 kg/m^3. Here all sides of the FGM plate are simply supported (SSSS) and a/h =10 and volume fraction index (k) taken as 5. Non dimensional frequencies of free vibration are tabulated in Table 4.2.a. It is observed that by modelling the FGM plate using 8×8 elements give quite accurate results taking considerably less computation time and computer memory. Hence 8 X 8 mesh is taken for further study.

Table 4.2a: Non dimensional frequencies for free vibrations of Al/Al$_2$O$_3$ FGM plates for different mesh sizes

Mesh size	2×2	4×4	% Error	6×6	% Error	8×8	% Error
Mode 1	4.2353	4.0631	4.065	4.0579	0.12798	4.0571	0.0197
Mode 2	12.4210	9.1291	26.50	9.0399	0.97709	9.0248	0.1670
Mode 3	12.4210	9.1291	26.50	9.0399	0.97709	9.0248	0.1670
Mode 4	24.7899	14.1335	42.986	13.8457	2.0362	13.8108	0.2520
Mode 5	24.7899	17.4286	29.694	16.7016	4.1713	16.5721	0.7753

4.3 Case Study:

In this section several free vibration analyses of square FGM plate have been performed for various parameters.

4.3.1 Case study

In this case the variation of natural frequencies for different a/h ratios for various volume fraction index (k) and support conditions are calculated for Al/Al$_2$O$_3$ square plate of dimension 1m X 1m. The support conditions are as follows:

Case-I : All sides simply supported (SSSS)

Case-II: All sides clamped (CCCC)
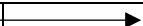
Case-III: One edge clamped; all other edges free (CFFF)

Case-IV: Two opposite edges clamped (CFCF)

First five modal frequencies in (Hz) are tabulated in Table 4.3.1.

Table 4.3.1: Frequencies (Hz)for free vibrations in Hz of Al/Al$_2$O$_3$ FGM plates for various support conditions

SSSS							
a/h	k →		0	0.5	1	5	10	Metal
		Mode 1	1681.20	1469.31	1364.93	1152.24	1075.56	855.70
		Mode 2	3680.8	3171.21	2868.55	2317.13	2201.17	1873.40
5		Mode 3	3680.8	3171.21	2868.55	2317.13	2201.17	1873.40
		Mode 4	5326	5326.	4199.63	3346.89	3154.23	2710.52

		0	0.5	1	5	10	Metal
	Mode 5	5827.04	5827.04	4818.47	3725.65	3446.20	2919.16
10	Mode 1	918.29	798.72	743.19	645.70	604.65	467.402
	Mode 2	2192.52	1877.07	1703.48	1436.35	1372.94	1115.96
	Mode 3	2192.52	1877.07	1703.48	1436.35	1372.94	1115.96
	Mode 4	3365.82	2893.98	2632.34	2198.06	2091.15	1713.15
	Mode 5	4113.22	3526.88	3189.51	2637.54	2519.47	2093.56
100	Mode 1	95.04	82.49	76.81	67.63	63.42	48.37
	Mode 2	237.70	202.54	184.08	159.60	153.20	120.99
	Mode 3	237.70	202.54	184.08	159.60	153.20	120.99
	Mode 4	380.96	325.06	295.94	256.69	245.97	193.90
	Mode 5	476.87	405.11	366.62	316.81	305.43	242.72

CCCC

a/h $\quad$ k		0	0.5	1	5	10	Metal
5	Mode 1	2566.67	2226.66	2020.15	1615.23	1524.62	1306.39
	Mode 2	4497.96	3926.54	3567.36	2791.43	2619.59	2289.27
	Mode 3	4497.96	3926.54	3567.36	2791.43	2619.59	2289.27
	Mode 4	5827.82	5276.45	4808.79	5932.76	3484.90	2919.84
	Mode 5	5827.82	5276.45	4808.79	5932.76	3484.90	2919.84
10	Mode 1	1568.28	1341.26	1211.77	1012.06	969.51	798.23
	Mode 2	2997.69	2576.53	2330.37	1913.96	1824.12	1525.78
	Mode 3	2997.69	2576.53	2330.37	1913.96	1824.12	1525.78
	Mode 4	4205.42	3624.83	3280.53	2668.66	2536.46	2140.49
	Mode 5	4976.34	4299	3892.81	3143.16	2980.55	2532.87
100	Mode 1	174.06	147.54	133.01	114.52	110.83	88.59
	Mode 2	356.99	302.78	273.04	234.79	227.08	181.70
	Mode 3	356.99	302.78	273.04	234.79	227.08	181.70
	Mode 4	537.68	457.16	412.79	353.35	340.96	273.67
	Mode 5	643.67	546.03	492.45	423.19	409.20	327.62

CFFF

a/h $\quad$ k		0	0.5	1	5	10	Metal
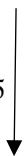
		0	0.5	1	5	10	Metal
5	Mode 1	321.86	273.44	246.55	210.24	202.93	163.82
	Mode 2	708.78	606.12	546.96	454.82	436.31	360.76
	Mode 3	1048.50	942	874	683.74	622.70	533.37
	Mode 4	1696.56	1455.21	1312.65	1075.73	1028.69	863.52
	Mode 5	2167.14	1851.28	1666.73	1379.90	1327.03	1103.03
10	Mode 1	165.28	140.12	126.30	108.54	105	84.12
	Mode 2	388.45	330.29	297.89	253.43	244.44	197.71
	Mode 3	968.39	823.90	742.90	629.61	606.87	492.90
	Mode 4	1048.97	941.64	872.78	681.42	621.15	533.83
	Mode 5	1228.87	1044.83	941.65	798.94	771.01	625.48
100	Mode 1	16.72	14.16	12.76	11.0049	10.65	8.51
	Mode 2	40.88	34.632	31.2136	26.89	26.04	20.80
	Mode 3	102.48	86.80	78.23	67.44	65.31	52.16
	Mode 4	130.793	110.792	99.8526	86.06	83.33	66.57
	Mode 5	148.74	126.016	113.57	97.85	94.74	75.71

CFCF

a/h $\quad$ k $\longrightarrow$		0	0.5	1	5	10	Metal
5 $\downarrow$	Mode 1	1695.86	1466.65	1329.6	1073.82	1016.49	863.17
	Mode 2	1924.08	1664.44	1507.12	1210.08	1146.86	979.33
	Mode 3	2819.35	2537.19	2348.47	1838.96	1676.82	1429.22
	Mode 4	3021.26	2602.39	2354.73	1894.68	1807.30	1537.75
	Mode 5	3875.60	3381.74	3071.37	2405.48	2258.88	1972.57
10	Mode 1	994.87	848.85	766.48	645.19	619.55	506.37
	Mode 2	1158.96	990.01	894.02	749.13	718.70	589.89
	Mode 3	1859.68	1589.09	1434.13	1197.59	1149.55	946.55
	Mode 4	2547.49	2187.14	1977.65	1630.13	1555.21	1296.63
	Mode 5	2758.81	2369.33	2142.16	1762.80	1673.39	1404.19
100	Mode 1	106.77	90.44	81.51	70.26	68.03	54.34
	Mode 2	127.10	107.67	97.04	83.62	80.96	64.69
	Mode 3	209.791	177.768	160.238	138.012	133.594	106.7809

	Mode 4	295	249.91	225.24	194.08	187.91	150.15
	Mode 5	323.79	274.32	247.24	212.99	206.20	164.80

4.3.2 Case study -2 (Al/ZrO₂)

In this case the variation of natural frequencies for different a/h ratios for various volume fraction index (k) and support conditions are calculated for Al/ZrO$_2$ square plate. The properties of ZrO$_2$ are E= 151×10^9 N/m^2, $\nu2$= 0.3 and ρ= 3800 kg/m^3.First five modal frequencies are tabulated in Table 4.3.2.

Table 4.3.2: Frequencies for free vibrations in Hz of Al/ZrO$_2$ FGM plates for various support conditions

SSSS							
a/h k ⟶		0	0.5	1	5	10	Metal
5 ↓	Mode 1	1192.75	1084.87	1039.68	957.7418	927.395	854.92
	Mode 2	2611.48	2366.67	2250.503	2052.422	1999.362	1871.814
	Mode 3	2611.48	2366.67	2250.503	2052.422	1999.362	1871.814
	Mode 4	3779.01	3435.57	3267.676	2956.488	2878.122	2708.654
	Mode 5	4199.99	3865.18	3671.862	3251.257	3149.591	3008.937
10	Mode 1	651.50	591.127	567.432	528.331	511.128	466.97
	Mode 2	1555.51	1404.64	1339.523	1242.796	1208.844	1114.933
	Mode 3	1555.51	1404.64	1339.523	1242.796	1208.844	1114.933
	Mode 4	2387.92	2160.24	2060.052	1901.784	1849.352	1711.581
	Mode 5	2918.18	2638.22	2511.861	2313.797	2252.72	2091.652
100	Mode 1	67.43	61.1152	58.708	54.927	53.117	48.332
	Mode 2	168.64	151.923	145.114	136.076	132.248	120.878
	Mode 3	168.64	151.923	145.114	136.076	132.248	120.878
	Mode 4	270.28	243.601	232.763	218.169	211.959	193.725
	Mode 5	338.32	304.490	290.564	272.529	265.079	242.498
CCCC							
a/h k ⟶		0	0.5	1	5	10	Metal
5 ↓	Mode 1	1820.967	1655.28	1574.275	1426.024	1387.877	1305.206
	Mode 2	3191.279	2909.32	2764.33	2479.656	2413.577	2287.395
	Mode 3	3191.279	2909.32	2764.33	2479.656	2413.577	2287.395
	Mode 4	4200.062	3873.38	3686.309	3260.335	3153.771	3009.001
	Mode 5	4200.062	3873.38	3686.309	3260.335	3153.771	3009.001
10	Mode 1	1112.633	1004.83	957.039	885.078	861.546	797.497
	Mode 2	2126.747	1925.04	1832.326	1681.683	1637.074	1524.379
	Mode 3	2126.747	1925.04	1832.326	1681.683	1637.074	1524.379
	Mode 4	2983.594	2704.13	2572.906	2351.117	2288.85	2138.537
	Mode 5	3530.544	3203.19	3046.893	2774.603	2701.159	2530.571
100	Mode 1	123.495	111.07	105.898	99.314	96.664	88.517
	Mode 2	253.276	227.852	217.238	203.596	198.153	181.539
	Mode 3	253.276	227.852	217.238	203.596	198.153	181.539

		0	0.5	1	5	10	Metal
	Mode 4	381.468	343.528	327.5	306.177	297.914	273.423
	Mode 5	456.659	410.86	391.712	367.005	357.191	327.318

CFFF

a/h	k ──────▶	0	0.5	1	5	10	Metal
5	Mode 1	228.35	205.6	195.94	183.01	178.16	163.67
	Mode 2	502.86	454.06	432.25	399.52	389.07	360.43
	Mode 3	744.26	685.94	653.25	577.85	558.29	533.45
	Mode 4	1203.65	1088.35	1035.22	951.24	926.68	862.73
	Mode 5	1537.51	1387.62	1320.06	1219.73	1188.54	1102.03
10	Mode 1	117.26	105.48	100.56	94.24	91.73	84.05
	Mode 2	275.6	248.22	236.55	220.7	214.84	197.54
	Mode 3	687.04	618.98	589.74	549.45	534.94	492.45
	Mode 4	744.3	685.76	652.88	577.51	558.13	533.49
	Mode 5	871.84	785.21	748.08	697.58	679.22	624.9
100	Mode 1	11.86	10.67	10.17	9.54	9.29	8.5
	Mode 2	29	26.08	24.87	23.33	22.71	20.79
	Mode 3	72.71	65.38	62.33	58.5	56.94	52.12
	Mode 4	92.79	83.44	79.55	74.65	72.66	66.51
	Mode 5	105.53	94.89	90.48	84.89	82.63	75.64

CFCF

a/h	k ──────▶	0	0.5	1	5	10	Metal
5	Mode 1	1203.15	1092.12	1039.09	945.61	920.31	862.38
	Mode 2	1365.07	1239.09	1178.22	1070.94	1042.75	978.43
	Mode 3	2007.73	1850.65	1762.21	1558.78	1506.37	1438.91
	Mode 4	2143.49	1941.82	1845.54	1684.79	1641.66	1536.38
	Mode 5	2749.66	2506.03	2381.09	2137.45	2080.64	1970.86
10	Mode 1	705.83	636.76	606.65	563.03	548.05	505.91
	Mode 2	822.24	742.15	706.91	654.88	637.5	589.35
	Mode 3	1319.37	1190.98	1134.06	1049.69	1022.06	945.68
	Mode 4	1807.34	1635.11	1556.57	1430.96	1392.99	1295.44
	Mode 5	1957.27	1770.97	1685.71	1548.82	1505.94	1402.9
100	Mode 1	75.5	68.11	64.94	60.94	59.32	54.29
	Mode 2	90.17	81.08	77.31	72.54	70.61	64.63
	Mode 3	148.84	133.85	127.62	119.71	116.52	106.68
	Mode 4	209.3	188.2	179.44	168.36	163.88	150.02
	Mode 5	229.72	206.57	196.95	184.77	179.85	164.65

4.4. Discussion on results:

4.4.1. Variation of natural frequency for different modes for varying power index k:

In this case variation of results is plotted for first five modal frequencies in Fig. 4.4.1a to 4.4.1h by considering a/h ratios 5 and 100 respectively for various volume fraction index (k) and support conditions.
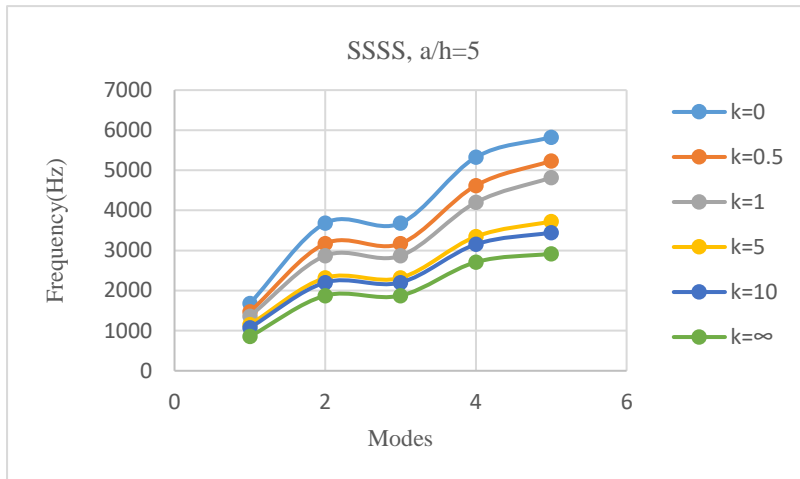
Fig 4.4.1a First five modal frequencies of Al/Al$_2$O$_3$ FGM plate in SSSS condition for different k values and a/h=5

Fig 4.4.1b First five modal frequencies of Al/Al$_2$O$_3$ FGM plate in SSSS condition for different k values and a/h=100
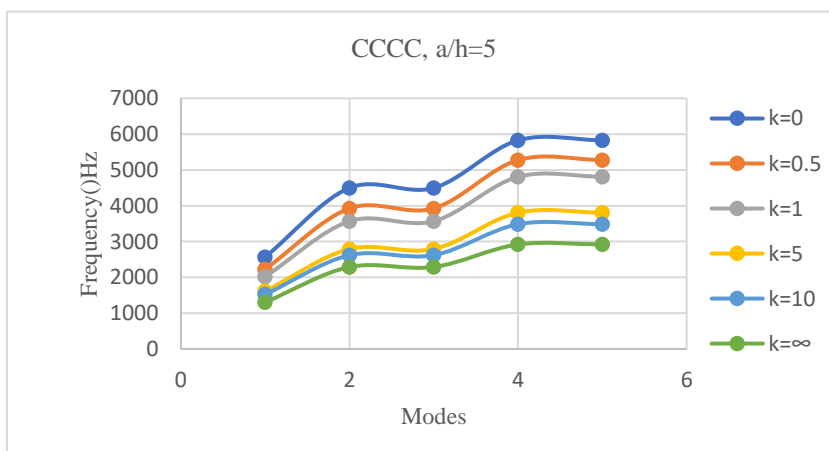

Fig 4.4.1c First five modal frequencies of Al/Al$_2$O$_3$ FGM plate in CCCC condition for different k values and a/h=5
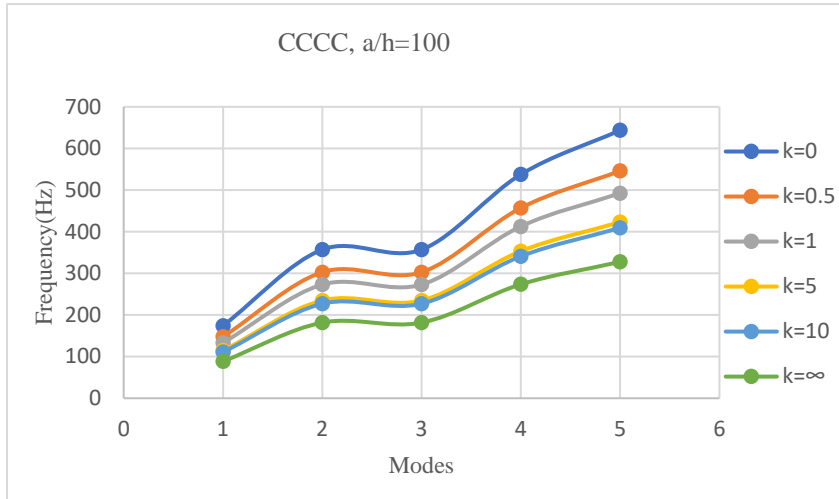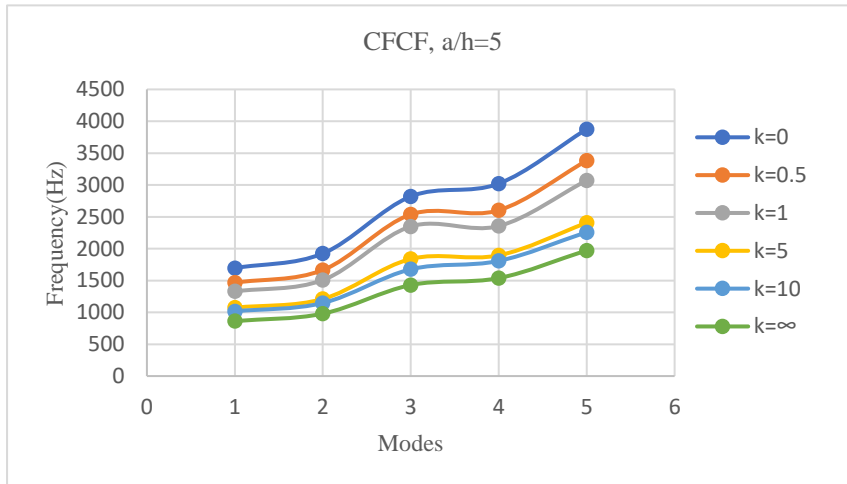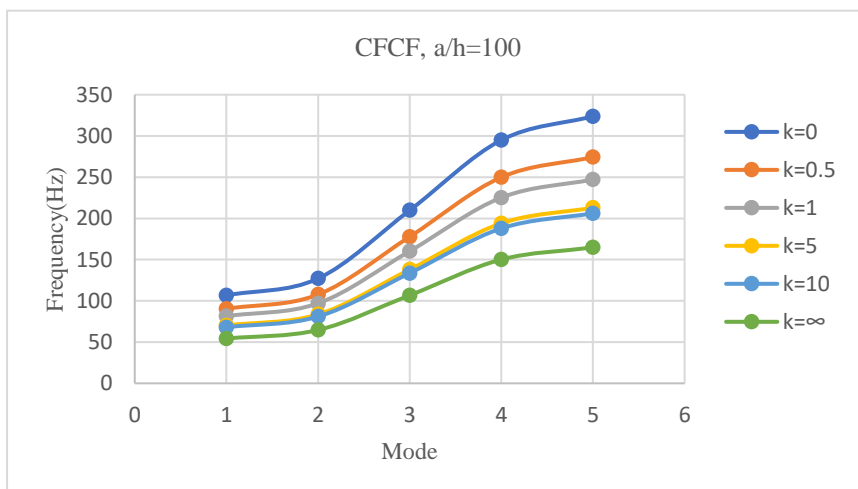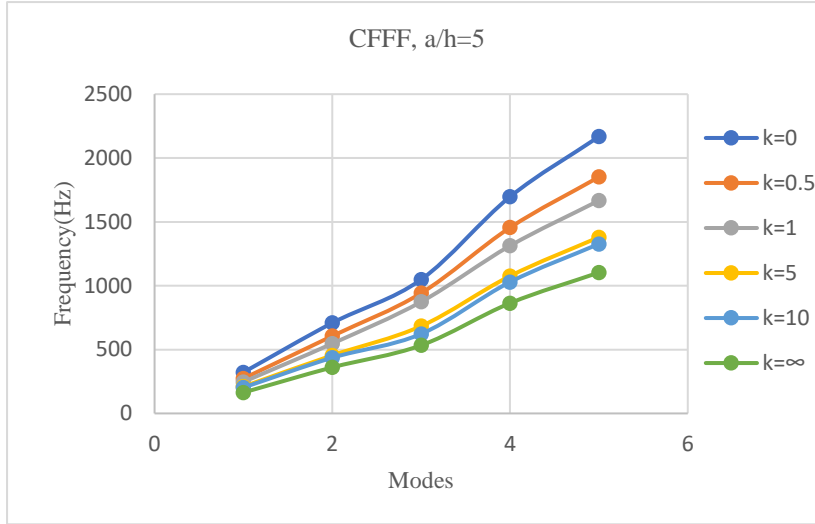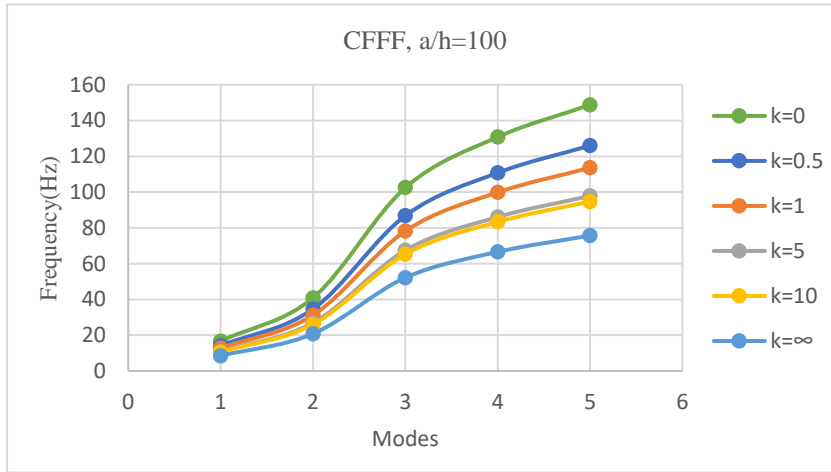
46

Fig 4.4.1d First five modal frequencies of Al/Al$_2$O$_3$ FGM plate in CCCC condition for different k values and a/h=100

Fig 4.4.1e First five modal frequencies of Al/Al$_2$O$_3$ FGM plate in CFCF condition for different k values and a/h=5

Fig 4.4.1f First five modal frequencies of Al/Al$_2$O$_3$ FGM plate in CFCF condition for different k values and a/h=100

Fig 4.4.1g First five modal frequencies of Al/Al$_2$O$_3$ FGM plate in CFFF condition for different k values and a/h=5

Fig 4.4.1h First five modal frequencies of Al/Al$_2$O$_3$ FGM plate in CFFF condition for different k values and a/h=100

Observations:

1) It is observed from Fig 4.4.1a to 4.4.1h that increase in a/h ratio from 5 to 100 results in a drastic decrease of fundamental frequency values in all five modes irrespective of 'k' values which means thicker FGM plates vibrate with higher frequencies and more vigorously than thinner plates. It is obvious as thicker plates have higher stiffness.

2) The 2nd and 3rd modal frequencies are same in SSSS and CCCC plates as the boundary conditions are symmetric. In CFCF case for a/h=5, the difference between 3rd and 4th mode frequencies are nominal compared to the case a/h=100. Also for CFFF case, the 2nd, 3rd and 4th mode reverses its direction when a/h increases from 5 to 100. For CCCC case when a/h=5, it is observed that the 4th and 5th modal frequencies are similar in magnitude, which is not seen for a/h=100. Hence, it can be said that thickness plays a very important role in the modal frequency.

3) Power index k=0 indicates ceramic, hence natural frequency is higher than k=10 which indicates more part of metal. Actually, k=∞ indicates pure metal i.e. aluminium.

4.4.2. Variation of natural frequency for varying length to side ratio (a/h):

In this case the variation of results with a constant volume fraction index (k) and varying a/h ratio namely a/h=5,10,100 is plotted for different support conditions in Fig. 4.4.2a to 4.4.2d. The power index k is kept constant at 1.
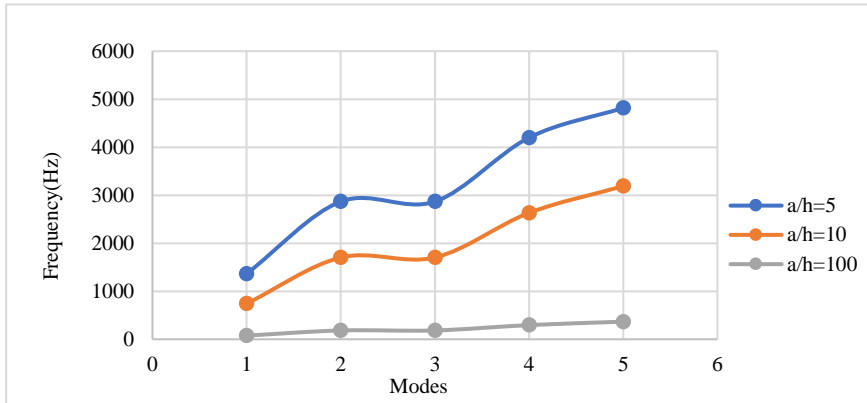

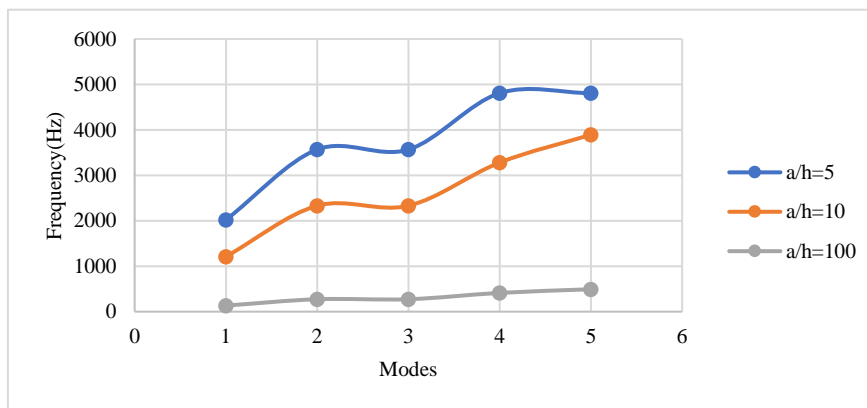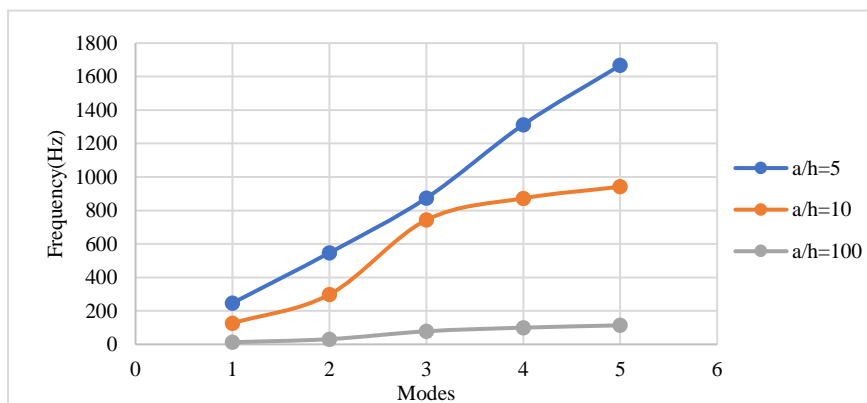Fig 4.4.2a First five modal frequencies of Al/Al$_2$O$_3$ FGM plate in SSSS condition for different aspect ratios and k=1

Fig 4.4.2b First five modal frequencies of Al/Al$_2$O$_3$ FGM plate in CCCC condition for different aspect ratios and k=1

Fig 4.4.2c First five modal frequencies of Al/Al$_2$O$_3$ FGM plate in CFFF condition for different aspect ratios and k=1
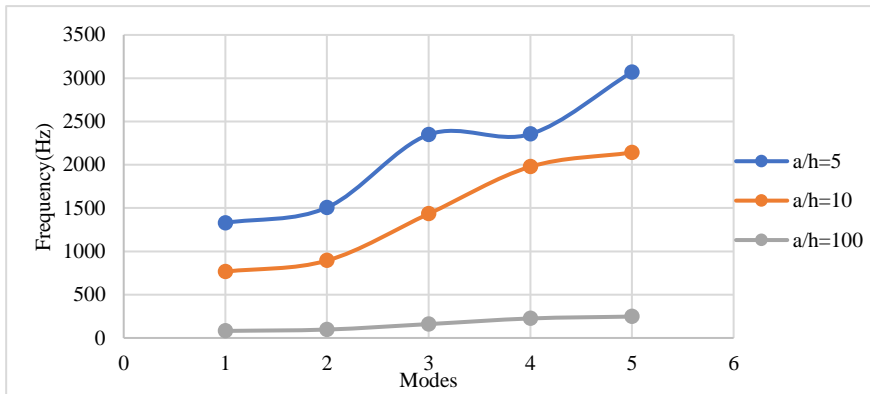
Fig 4.4.2d First five modal frequencies of Al/Al$_2$O$_3$ FGM plate in CFCF condition for different aspect ratios and k=1

Observations:

It is observed that for a/h=100, the changes in natural frequency for different modes are nominal and generally follows a straight line pattern. Effect of thickness become prominent for boundary condition CFCF and CFFF and the pattern changes as shown in Fig. 4.4.2c and 4.4.2d. The 3rd mode frequency nearly matches for a/h=10 and a/h=5 for CFFF case.

4.4.3. Variation of natural frequency for various volume fraction index (k) and boundary condition

A comparative graphical study has been carried out for Al/Al$_2$O$_3$ in Fig. 4.4.3a to 4.4.3c for first mode frequencies for different 'k' values keeping constant aspect ratios of 5,10 and 100 respectively for different support conditions namely SSSS, CCCC, CFFF and CFCF.
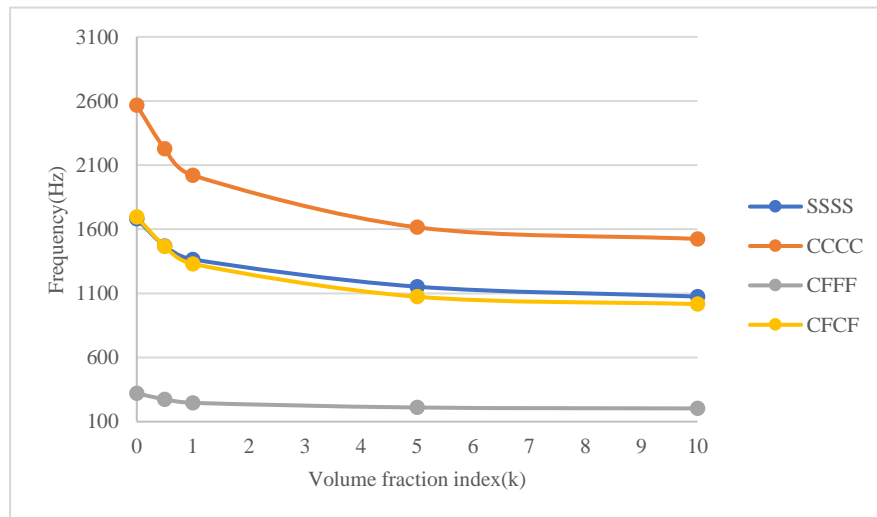
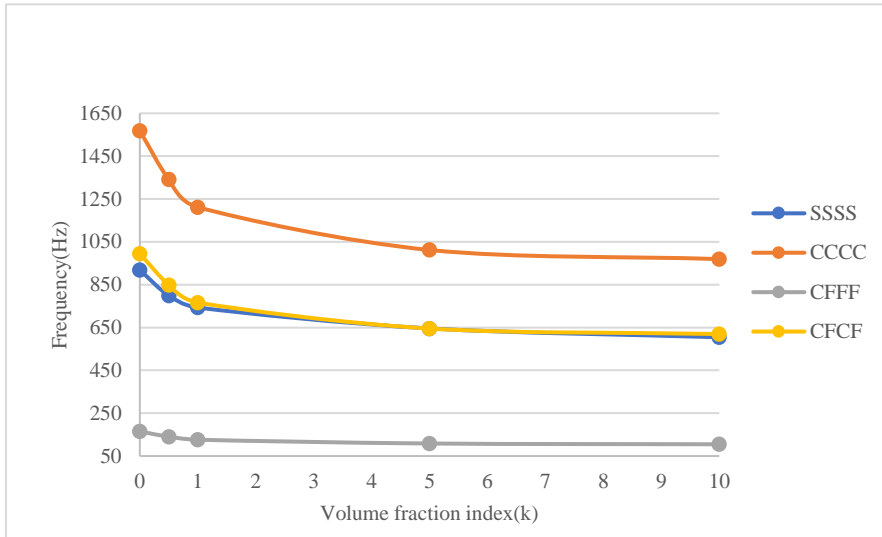Fig 4.4.3a First mode frequency of Al/Al$_2$O$_3$ FGM plate for different boundary conditions and a/h=5

50

Fig 4.4.3b First mode frequency of Al/Al$_2$O$_3$ FGM plate for different boundary conditions and a/h=10
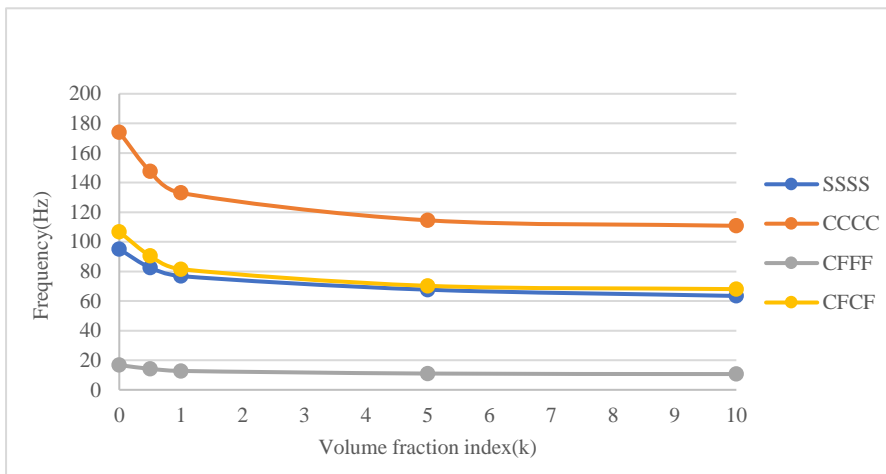

Fig 4.4.3c First mode frequency of Al/Al$_2$O$_3$ FGM plate for different boundary conditions and a/h=100

Observation:

1) First mode frequencies decrease exponentially with the increase of volume fraction index (k) for all types of FGM plates

2) CFCF and SSSS plates vibrate with almost similar magnitude of first mode frequencies for all a/h ratios.

3) Clamped (CCCC) plates vibrate with highest frequency whereas cantilever (CFFF) with lowest magnitude of frequency values. This is because the degree of restraint is much more for CCCC case than in CFFF case. Actually, the stiffness of a structure depends on its degree of restraint. More the restraint, more is the stiffness.

4) Variation of first mode frequencies is distinct for all types of FGM plates for lower values of volume fraction index (k) namely k=0, k=0.5 and k=1. This is because with change in values of "k" the proportion of metal increases and proportion of ceramic reduces. The effect of reduction in ceramic is prominent for lower "k" values.

4.4.4. Variation of natural frequency for different materials (Al/Al$_2$O$_3$ and Al/ZrO$_2$)

A comparative graphical study has been carried out for Al/ZrO$_2$ in Fig. 4.4.4a to 4.4.4c for first mode frequencies for different 'k' values keeping constant a/h of 5,10 and 100 respectively for different support conditions namely SSSS, CCCC, CFFF and CFCF.

Observations:

1) From Table 4.3.1 and 4.3.2, it is observed that plates made up of Al/Al$_2$O$_3$ as FGM vibrate with higher magnitude of frequencies than Al/ZrO$_2$ FGM plates. This is because the ceramic Al$_2$O$_3$ has higher modulus of elasticity than that of ZrO$_2$.

2) Fig. 4.4.4a to 4.4.4c shows that a sharp distinction in first mode natural frequency is present in case of Al/ ZrO$_2$ FGM plates for higher values of length to thickness ratios (a/h=10 and 100) for SSSS and CFCF condition. This distinction is present in case of Al/Al$_2$O$_3$ FGM plate only for lower 'k' values (refer Fig. 4.4.3a to 4.4.3c).
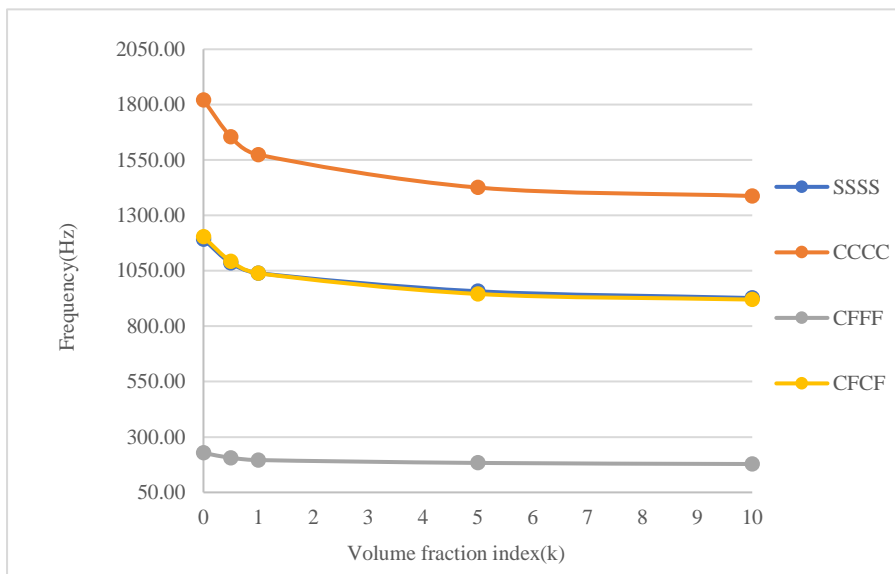

Fig 4.4.4a First mode frequency of Al/ ZrO$_2$ FGM plate for different boundary conditions and a/h=5
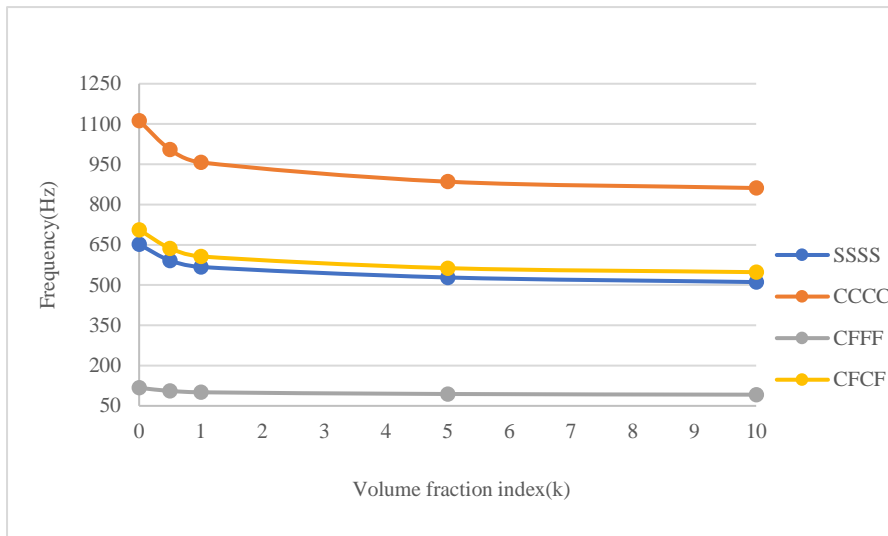
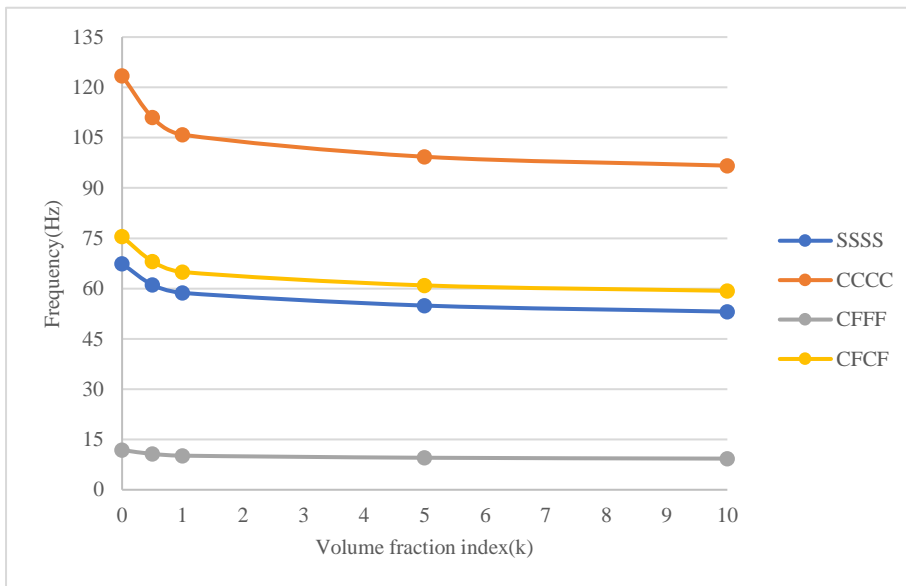Fig 4.4.4b First mode frequency of Al/ ZrO_2 FGM plate for different boundary conditions and a/h=10


Fig 4.4.4c First mode frequency of Al/ ZrO_2 FGM plate for different boundary conditions and a/h=100

4.5. Mode shapes for simply supported (SSSS) square Al/Al$_2$O$_3$ plate for k=1 and a/h=100
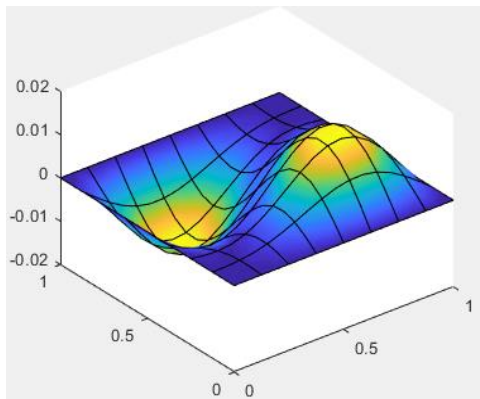
First five mode shapes are drawn for Al/Al$_2$O$_3$ plate (SSSS) for k=1 and a/h=100 It is observed that the 1st, 4th and 5th mode are symmetrical bending mode whereas 2nd and 3rd mode are antisymmetric bending mode.
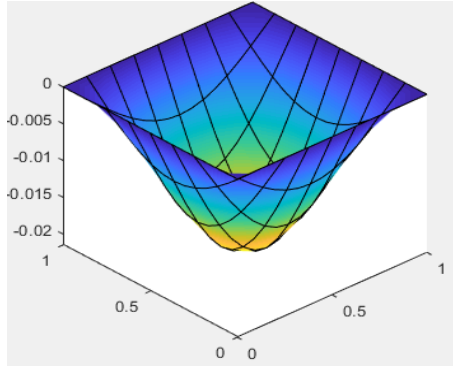
1st mode shape
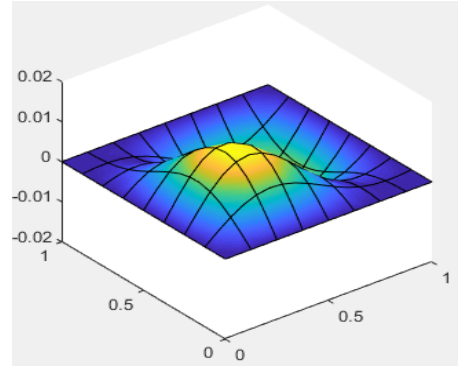
2nd mode shape

3rd mode shape
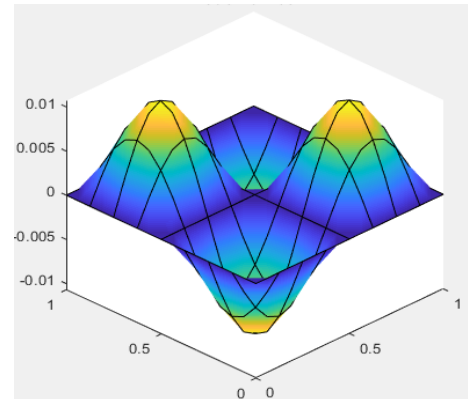
4th mode shape
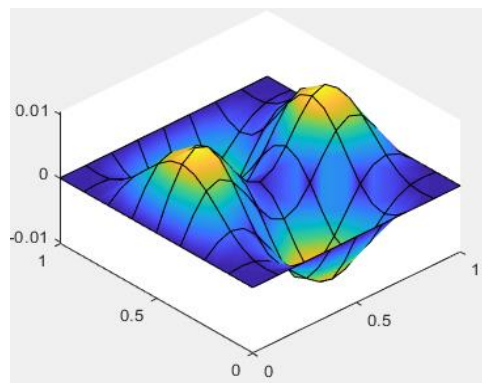
5th mode shape

Fig 4.5: First five mode shapes of Al/Al$_2$O$_3$ FGM plate under HSDT

Chapter 5

5.0 Conclusion

In our thesis free vibration analysis of functionally graded plates using higher order shear deformation theory (HSDT) have been discussed using a MATLAB program. The material property i.e., Young's modulus and density varies along thickness direction following power law variation. Eight noded serendipity plate finite elements with seven degrees of freedom per node have been used in the analysis. Parametric studies have been conducted by incorporating variation of support conditions, volume fraction index, a/h ratios and material properties.

From the parametric studies, it is observed that

1) The thickness plays a very important role in dynamic analysis of plates. The behavior of thick plate with side to thickness ratio a/h=5 is quite different at different modes than the thin plate with a/h=100.
2) It is observed that increase in the number of restraints increases stiffness of the structure thus increasing its natural frequency.
3) With increase in power law index k, the proportion of metal increases thus reducing its stiffness.
4) When material is changed the stiffness varies depending on the elastic properties of the constituent materials. But the pattern of variation in frequency for different boundary conditions and thickness are similar.

The behaviour of FGM plate structure depends on a number of variables. The most important variations are the boundary conditions and different a/h ratio and face materials. Hence for use of FGM plate structures in practice, physical experiment is necessary. But it will be costly and generate huge non-biodegradable waste. Hence numerical experiments are necessary to get the behaviour pattern of FGM plate structures and then physical experiment should be done based on selected numerical results before using it practically.

5.1 Scope of future study

1. In this program, 8 noded serendipity elements are used to model the plate. One can use 9 noded Lagrangian plate finite elements to model the plate to see the changes in stiffness.
2. Here third order shear deformation theory has been used, one can use other higher order theories for plate analysis like parabolic, hyperbolic, elliptical or trigonometric theories.
3. In this study, only flat plate elements are used. The program can be extended for shell elements too.
4. Only free vibration analysis of FG plates have been performed. The program can be extended to investigate dynamic and forced vibration behaviour.
5. Here in this program only selected materials Al/ZrO_2 and Al/Al_2O_3 have been used. The behaviour of other materials can also be investigated.

Chapter 6

6.0 References

1. Vibration of functionally graded beams and plates by Snehashis Chakraverty and Karan Kumar Pradhan(2016)

2. Analysis of functionally graded plates using higher order shear deformation theory by - M.N.A. Gulshan Taj, Anupam Chakrabarti , Abdul Hamid Sheikh(Applied Mathematical Modelling (Volume 37, Issues 18–19, 1 October 2013, Pages 8484-8494)

3. A simple four-unknown refined theory for bending analysis of functionally graded plates by Ashraf M. Zenkour(Applied Mathematical Modelling,Volume 37, Issues 20–21, 1 November 2013, Pages 9041-9051)

4. Some analytical solutions of functionally graded Kirchhoff plates by Andrea Apuzzo, Raffaele Barreta and Raimondo Luciano(Composites Part B: Engineering,Volume 68, January 2015, Pages 266-269)

5. Static behaviour of functionally graded sandwich beams using a quasi-3D theory by Thuc P.Vo , Hu Tai-Thai , Trung Kien Nangyuen , Fawad Inam(Composites Part B: Engineering) Volume 68, January 2015, Pages 59-74)

6. A new hyperbolic shear deformation theory for bending and free vibration analysis of isotropic, functionally graded, sandwich and laminated composite plates by – Amale Mahi , El Abbas Adda Bedia , Abdelouahed Tounsi(Applied Mathematical Modelling) Volume 39, Issue 9, 1 May 2015, Pages 2489-2508)

7. Static and free vibration analyses of carbon nanotube-reinforced composite plates using finite element method with first order shear deformation plate theory by – PingZhu , Z.X.Lei , K.M.Liew(Composite Structures,Volume 94, Issue 4, March 2012, Pages 1450-1460)

8. Free vibration analysis of functionally graded carbon nanotube-reinforced composite cylindrical panel embedded in piezoelectric layers by using theory of elasticity by Alibeigloo (European Journal of Mechanics - A/Solids) Volume 44, March–April 2014, Pages 104-115

9. Static response and free vibration analysis of FGM plates using higher order shear deformation theory by Mohammad Talha, B.N. Singh (Applied Mathematical Modelling 34 (2010) 3991–4011)

10.   Analysis of functionally graded plates by J.N Reddy, INTERNATIONAL JOURNAL FOR NUMERICAL METHODS IN ENGINEERING Int. J. Numer. Meth. Engng. 47, 663-684(2000)